Single point mutations in type IV pilus fiber proteins restore twitching in *ΔpilU* mutants

Single point mutations in type IV pilus fiber proteins restore twitching in *ΔpilU* mutants

By REBECCA HELEN BARNSHAW, BSc.

A Thesis Submitted to the School of Graduate Studies in Partial Fulfillment of the Requirements for the Degree Master of Science

McMaster University MASTER OF SCIENCE (2022)

Hamilton, Ontario (Biochemistry and Biomedical Science)

TITLE: Single point mutations in type IV pilus fiber proteins restore twitching in *ΔpilU* mutants

AUTHOR: Rebecca H. Barnshaw, BSc. (University of Guelph)

PROFESSOR: Dr. Lori L. Burrows

NUMBER OF PAGES: xiii, 66

LAY ABSTRACT

Pseudomonas aeruginosa is a bacterium that causes serious infections. *P. aeruginosa* uses adhesive, "grappling hook" filaments called Type IV pili (T4P) to stick to its hosts. T4P can be repeatedly extended and retracted, allowing the bacteria to crawl on surfaces (twitching) but making them susceptible to bacteriophages, viruses that attach to pili then kill the bacterial cells. The motor proteins PilT and PilU are required for twitching, but only PilT is essential for phage killing, implying that pili are retracted even when PilU is missing. Here we hypothesized that PilU is important for twitching because it helps generate force for retraction when pili are under tension. We isolated multiple mutations in pilus components that restored twitching in the absence of PilU, and propose that these mutations allow for easier retraction of pili. This information helps us understand how T4P help the bacteria to spread during infection.

ABSTRACT

Type IV pili (T4P) are long adhesive surface filaments produced by bacteria and are a key virulence factor for many pathogens. T4P are produced by a dynamic intracellular nanomachine that facilitates the assembly (extension) and disassembly (retraction) of pili. Pilus dynamics are enabled by the motor subcomplex of the nanomachine, where cytoplasmic ATPases power pilus assembly (PilB) and disassembly (PilT and PilU). In many, but not all, T4P expressing bacteria – including our model organism *Pseudomonas aeruginosa* – two retraction ATPases are required for functional retraction, which can be assessed by measuring twitching motility. Deletion of *pilT* results in loss of twitching and phage susceptibility (another hallmark of pilus function) while deletion of *pilU* results in loss of twitching but retention of phage susceptibility, indicating pili can still be retracted. We hypothesized that PilU adds to the force of pilus retraction, facilitating disassembly when the fiber is under tension. We mutated *ΔpilU* and *pilU::Tn5* strains with ethyl methanesulfonate and screened for gain-of-twitching mutants. Whole genome sequencing revealed multiple point mutations in the major pilin protein PilA or the pilus adhesin, PilY1. These point mutations were recapitulated in a *ΔpilU* strain and restored twitching to varying degrees. Complementation of *pilA* point mutants with *pilU in trans* influenced the twitching zone of only one mutant, and *in trans* expression of wild-type *pilA* resulted in a significant reduction in twitching in most. The contribution of PilU to the force of pilus retraction was further investigated by a polyacrylamide micropillar assay, where no pulling events could be detected for either

ΔpilT or *ΔpilU* mutants. Exopolysaccharide production, a proxy for surface sensing, was uncoupled from twitching motility in the *pilA* point mutants. These results are a significant step forward to understanding what PilU does and, provides insight to the dynamics of the pilus fiber.

ACKNOWLEDGMENTS

Thank you Dr. Burrows for accepting me as a student and facilitating the completion of this degree. Thank you to my committee members Dr. Whitney and Dr. Howell, your evaluations have helped me progress and learn.

It is not hyperbolic to say the success of every Burrows lab project rests on Hanjeong Harvey. You have been steadfast in your commitment to student success academically and personally. Your scrupulous criticisms have greatly improved my capabilities as a researcher and presenter, and your encouragement gave me the confidence to continue. Thank you.

Thank you Ikram, Luke, Nathan, and Veronica for your companionship throughout this degree. It has made the late nights and early mornings bearable, and lab meetings entertaining. I wish this degree was completed under different circumstances, that I would have gotten to know you all better.

Thank you to my family. We have been strained the past few years, but I still love you. Thank you mum for the late-night chats talking my confidence up, and talking me down from my frustration. Thank you Anthony for all your love in the form of baked goods, memes, and justified criticisms of my apartment. I hope you are happy that I have finally moved. Thank you dad for being there, patient, cautious not to transgress. Through this degree you have been there for me when I needed you. Thank you to my grandparents, aunts, uncles and cousins for all your support, I love you all.

Thank you to my friends Pooja, Alano, Carlos, Daniel, Sarah, Colin, Manali, Ben, Daniella, Fran and Gemma for your unwavering encouragement and support. Thank you Ayan and Anika for your support and comfort through the trials of navigating an institution built entirely for the exclusion of our likes.

Thank you Dhanyasri. These words will never be enough to thank you for the friendship you have given and the home you have provided. This degree would not have been possible if not for you. I am forever grateful that, however unfortunate the circumstance, I met you.

This is my degree earned on island time, for my family, and for my community.

We likkle but tallawah

TABLE OF CONTENTS

LIST OF FIGURES

Supplementary figures

LIST OF TABLES

LIST OF ABBREVIATIONS

AMIN	Amidase N-terminal
ASCE	Additional strand catalytic 'E'
ATP	Adenosine triphosphate
BACTH	Bacterial two-hybrid
BCIP	5-Bromo 4-Chloro 3'-Indolyphosphate p-Toluidine salt
cAMP	Cyclic adenosine monophosphate
CC	Coiled-coil
CD	Circular dichroism
c-di-GMP	Cyclic-di-guanosine monophosphate
cryoET	Cryo-electron tomography
C-terminal	Carboxyl-terminal
DNA	Deoxyribonucleic acid
diH_2O	Deionized H_2O
EMS	Ethyl methanesulfonate
EPS	Exopolysaccharide
Gm	Gentamicin
H	Hour(s)
IM	Inner membrane
iSCAT	Interferometric scattering microscopy
kDa	Kilodalton
LB	Luria-Bertani broth
MALLS	Multi angular laser light scanning
MCPs	Methyl-accepting chemotaxis proteins
MIC	Minimum inhibitory concentration
NBT	Nitrotetrazolium Blue Chloride
NMR	Nuclear magnetic resonance
N-terminal	Amino terminal
OD	Optical density
OM	Outer membrane
PBS	Phosphate buffered saline
PCR	Polymerase chain reaction
pH	Power of hydrogen
pN	Pico newton
PoMP	Polyacrylamide micropillar assay
RR	Response regulator
Sulfo-SANPAH	Sulfosuccinimidyl 6-(4'-azido-2'-nitrophenylamino)hexanoate
SDS	Sodium dodecyl-sulfate
SEC-MALS	Size exclusion chromatography and multi-angle light scattering
SK	Sensor kinase
TCS	Two-component system

TPR	Tetratricopeptide
T4P	Type IV pili
T2SS	Type II secretion system
TIIISS	Type III secretion signal
Vfr	Virulence factor regulator
vWA	von Willebrand A-like
WB	Walker B
WA	Walker A
WT	Wild type

DECLARATION OF ACADEMIC ACHEIVEMENT

Hanjeong Harvey generated the *P. aeruginosa* PAO1 *ΔfliC* strain, and pBADGr-*pilA* construct.

The EMS mutagenesis protocol was developed with the insight of Dr. Marie Elliot.

Veronica Tran performed the phage susceptibility assays. Nathan Roberge constructed the *P. aeruginosa* PAO1 *ΔpilU pilY1* point mutants and completed the corresponding twitching assays. Ikram Qaderi constructed the pBADGr-*pilA* A40 substitution constructs and performed the twitching assays.

The *P. aeruginosa* PAO1 *ΔpelF* and *ΔpelA* mutants were provided by Dr. Lynne Howell, who also provided information and critiques for the Congo red assay.

The polyacrylamide micropillar (PoMP) assay was performed by Dr. Nicolas Biais and Nicolas Pellet. The PoMP data was analyzed and summarized by Nicolas Pellet.

I performed the remaining work for this thesis unless otherwise stated.

CHAPTER 1. INTRODUCTION

Type IV pili (T4P) are long adhesive surface filaments produced by both bacteria and archaea, suggesting an ancient origin of the T4P system [1,2]. The pilus filament is a helical polymer of protein monomers that can be repeatedly extended (assembled) and retracted (disassembled) by a complex intracellular nanomachine. Extension and retraction is essential to T4P function; this ability is exploited by bacteria and archaea for functions such as twitching motility, biofilm formation, cell-cell and cell-host adhesion, surface sensing, and natural competence for DNA uptake [2–4]. The ubiquity and versatility of T4P contribute to pathogenesis, making them an important virulence factor as well as a key component in bacterial and archaeal physiology. Despite this, many details of the mechanics of the T4P nanomachine remain unknown.

1.1 Type IV pili overview

The pilus filaments are the surface-exposed component of the large nanomachine that builds them. The dynamic multi-component nanomachine spans the entirety of the cell envelope and can be divided into four subcomplexes, including the pilus itself (**Figure 1**). The others are the secretin, alignment subcomplex, and motor subcomplex. The motor subcomplex polymerizes pilin monomers during pilus extension and facilitates their return to the inner membrane during retraction. The secretin forms a gated pore in the outer membrane, allowing pilus extension to the external environment. The motor subcomplex and the secretin are connected by the alignment subcomplex to ensure that the pilus extending through the periplasm exits the secretin[5].

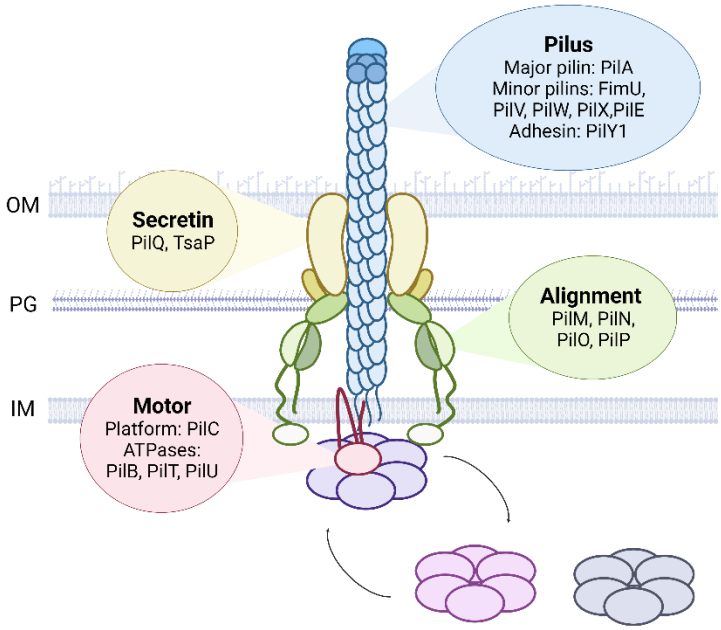

Figure 1. The T4P nanomachine of *Pseudomonas aeruginosa.* The secretin complex (Q) creates a pore in the outer membrane allowing the pilus fiber (A) to exit the cell. The inner membrane alignment complex (M,N,O,P) connects the secretin to the motor complex (B, C, T, U). The motor complex platform (C) in the inner membrane polymerizes and depolymerizes the pilus fiber via its interaction with the extension (B) and retraction (T,U) ATPases.

1.2 The pilus

A single pilus fiber can contain hundreds to thousands of protein monomers of the major pilin subunit, PilA [6]. Repeating PilA monomers form the length of the pilus, while the minor pilin subunits – FimU, PilV, PilW, PilX, PilE, and the non-pilin protein PilY1 – form a priming complex [7,8]. The minor pilin complexes are localized at the tip of each pilus as PilA monomers are added below them, and are present in lower abundance compared to PilA [7–9]. Together the major and minor pilin subcomplexes form a helical fiber up to several microns long and 6-9 nm in diameter, yet capable of

withstanding retraction forces of >100pN [10,11]. This force is sufficient to displace 10,000 x the mass of a single cell [12].

Pilin proteins range between ~15-30 kDa and have three shared characteristics; a type III signal sequence that is removed prior to assembly by a prepilin peptidase, with simultaneous *N*-methylation of the new N-terminus; a conserved hydrophobic S-shaped N-terminal helix; and in most, a pair of Cys residues near the carboxy terminus that form a disulphide bond [11] . The general shape of a pilin is comparable to a lollipop. A pilin has an extended N-terminal α-helix, α1, of approximately 54 amino acids. It can be further divided into two sections; 1) the N-terminal half of the helix (α1N) which protrudes from the protein and in an assembled pilus fiber, forms the hydrophobic helical bundle at its core, and 2) the C-terminal half of α1 (α1C) which is embedded in a globular domain and interacts with a four- to five- stranded anti-parallel β-sheet that is linked to the C-terminus of the pilin via the disulphide bond [11,13] (**Figure 2**). The α1N portion can be considered the "stick" portion of the pilin lollipop. The "candy" portion is a globular C-terminal series of four- to five anti-parallel β-strands [11,13]. A flexible αβ-loop connects α1C to the first β-strand[11,13]. The last β-strand is connected to the D-region, which forms a loop enclosed by the conserved Cys residues (**Figure 2**)[13]. The sequences of the αβ-loop and D-region help determine the shape and chemistry of the pilus, and consequently its function. While the α1N region is highly conserved in T4P, the C-terminal regions that form the surface of the pilus are more variable; thus, molecular modeling of pilins on existing structural templates can be challenging. Major and minor

pilins are both processed by the prepilin peptidase PilD that cleaves the type III signal sequence and methylates the new N-terminus, then stored in the inner membrane when not assembled [14]. For PilA from *P. aeruginosa* PAO1, the model organism for this work, PilD cleaves six residues, resulting in a mature 15 kDa protein of 143 amino acids[9,15,16].

The only non-pilin associated with the pilus fiber is PilY1. It is a large ~125 kDa protein hypothesized to be processed by signal peptidase 1, separate from the processing of prepilins by PilD [14]. It may act as an adhesin, a mechanosensor involved in surface sensing and biofilm development, and/or as a plug that prevents complete retraction of the pilus filament into the cell. Its proposed role as a mechanosensor is based on the presence of a von Willebrand A (vWA)-like mechanosensory domain – similar those in eukaryotes – in its N-terminal region. PilY1 is necessary for increasing the second messenger cyclic-diguanylate-monophosphate (c-di-GMP), which promotes exopolysaccharide production (EPS) and downregulates flagellar motility, following surface encounters[17,18]. This pathway is thought to result from unfolding of the vWA domain upon surface contact, but the mechanism of signal transduction is poorly understood[17,19]. PilY1 and the minor pilins are essential for pilus assembly in model organisms such as *P. aeruginosa, Myxococcus xanthus, Neisseria gonorrhoeae* and *N. meningitidis* [7,8].

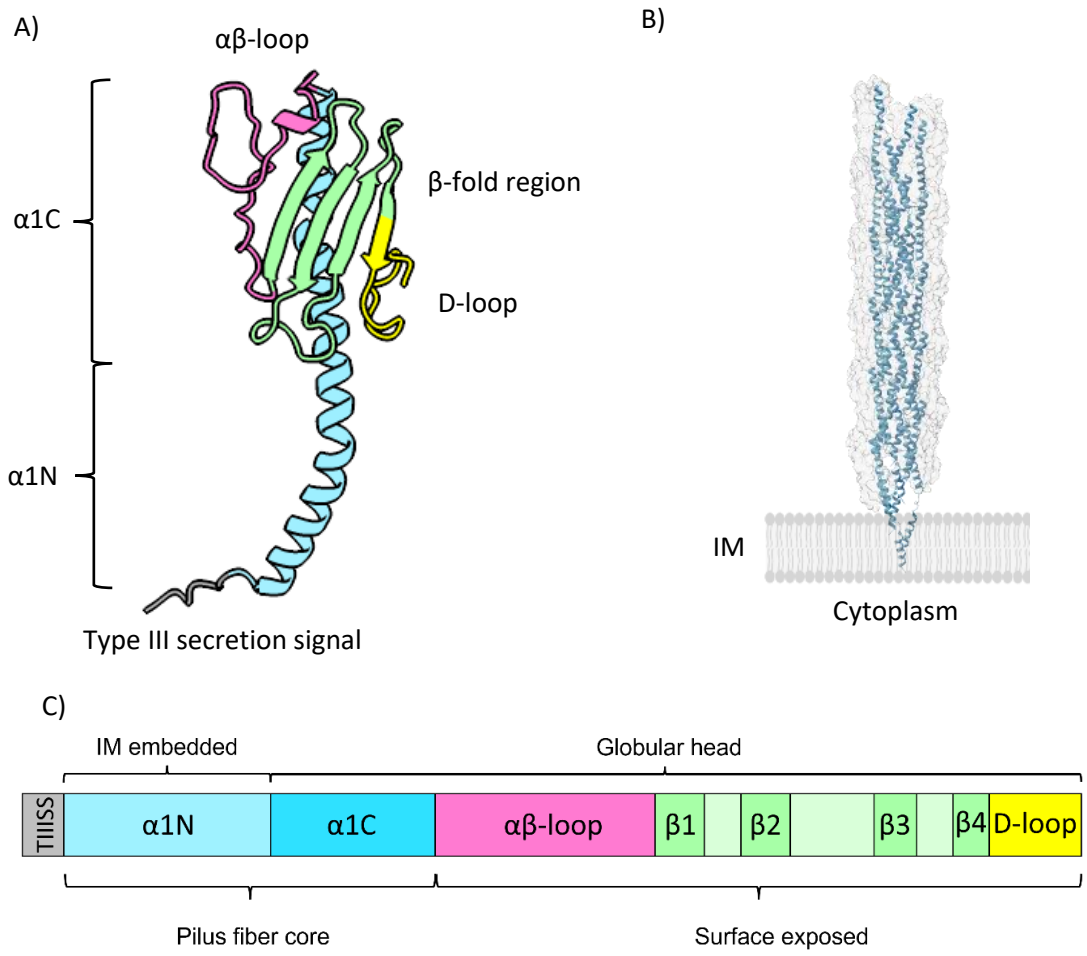

Figure 2. Pilus structure, and pilin monomer model with a linear representation. A) An AlphaFold 2 model of the *P. aeruginosa* PAO1 prepilin[21,22]. The six residue N-terminal type III secretion signal is coloured gray. The α1 region is coloured blue and divided into two sections; the α1N component forms the core of the pilus fiber and is inserted into the IM when the fiber disassembles, the α1C component is in the globular head region and interacts with the β-sheet. The αβ-loop is coloured pink, and the D-loop is coloured yellow. This figure is based on models and structures from Giltner et al. (2012) and Jacobsen et al. (2020)[1,23]. B) Cartoon of assembled *P. aeruginosa* PAK pilus fiber, the N-terminus α1 region is coloured blue and C-terminus globular head region is coloured grey (PDB: 5VXY)[20]. C) A linear representation of the *P. aeruginosa* PAO1 prepilin peptide.

The extreme mechanical strength of the pilus is due to extensive hydrophobic interactions between the conserved N-terminal α-helices of assembled pilin subunits [11]. Subunit-subunit interactions are also facilitated by complementary variable regions in the globular head domains. In a pilus fiber, the globular head region is the main surface-exposed region. Variability in the globular region also provides functional flexibility [11]. For example, positively-charged residues on the pilus surface can bind DNA to promote natural competence [24].

The production of major and minor pilins and PilY1 is tightly regulated by multiple signal transduction systems, including PilSR, the Pil-Chp system, and AlgR-FimS [18,25–27]. The PilSR two-component system (TCS) controls PilA expression [25,26]. The PilS sensor kinase detects the N-terminus of PilA within the IM through direct interaction with its six transmembrane segments [25,28]. The absence of PilA interactions trigger PilS to auto-phosphorylate at the cytoplasmic residue H319; this phosphate is then transferred to PilR D54[6,25,29–32]. PilR is the cytoplasmic response regulator, that with alternate sigma factor RpoN (σ^{54}), facilitates RNA polymerase binding to the *pilA* promoter to activate transcription[25,33]. Conversely, when PilA levels in the IM are high, PilS is proposed to act as a phosphatase to de-phosphorylate PilR and reduce *pilA* expression. PilS has a canonical phosphatase motif ExxN at position 320-323 adjacent to H319, and PilS overexpression reduces PilA expression, supporting a PilS phosphatase model [30].

The AlgR-FimS TCS regulates expression of the minor pilin operon [18,27]. FimS is

the sensor kinase and AlgR is the response regulator [16]. AlgR-P binds upstream of *fimU* and promotes transcription of the *fimU-PilVWXY1Y2E* operon [16]. AlgR-FimS also promotes the transcription of alginate synthesis genes, a key component of biofilms [16]. Minor pilin production can also be increased through activation of the Pil-Chp system, which like the T4P machinery is localized to the poles of the cell [34,35]. Through an unknown mechanism, this system reports on surface interactions of pili. The membrane bound methyl-accepting chemotaxis protein (MCP) PilJ undergoes a conformational change that is transmitted through an adaptor protein, PilI, to trigger autophosphorylation of ChpA (PilL) [17,18,36,37]. Phospho-ChpA then phosphorylates the cytoplasmic regulator PilG, which promotes activity of the adenylate cyclase, CyaB [38,39]. CyaB synthesizes cyclic adenosine monophosphate (cAMP), which binds the virulence factor regulator (Vfr) to promote transcription of the minor pilin operon and genes associated with EPS production[34,35].

1.3 The motor subcomplex

The motor subcomplex in most T4P-expressing bacteria consists of the platform protein, PilC, and two ATPase motors, PilB and PilT. In some species – including *P. aeruginosa* – there are multiple retraction ATPases, such as the ATPase PilU, however, their specific function(s) and location in the T4P machinery are unknown. My work addressed these questions.

PilC is an IM protein with 3 transmembrane domains connecting two cytoplasmic

bundles of 6 helices each, and acts as the interface between the cytoplasmic motor ATPases and the membrane-embedded pilins [40]. *Thermus thermophilus* PilC was initially suggested to be a dimer based on size exclusion chromatography and multi-angle light scattering (SEC-MALS) analyses. However, this stoichiometry disagrees with more recent structural data for the ATPase motors, coupled with cryoelectron tomography (cryo-ET) data that suggest a PilC dimer would be too large to fit into the central cavities of ATPase hexamers [20,41,42]. PilC interacts in the membrane with pilin subunits through their hydrophobic N termini, and with the ATPases through its cytoplasmic domains [40]. Pulldown data confirmed that the cytoplasmic N-terminal domain of PilC interacts with the polymerization ATPase, PilB [40]. In contrast, the details of PilC's association with the depolymerization ATPase PilT are less clear. Double point mutants of solvent-exposed residues in PilC's C-terminal cytoplasmic domain make the cells hyperpiliated and less motile relative to wild type, suggesting that the C-terminal domain may be involved in disassembly [40]. From those data, it was inferred that the cytoplasmic C-terminal domain of PilC might interact with the depolymerization ATPase, PilT [40].

The cytoplasmic alignment subcomplex protein PilM is proposed to form a 14-membered ring surrounding PilC's cytoplasmic domains, creating a socket for the ATPases and acting as a stator. This configuration would immobilize the ATPases during the conformational changes that they undergo upon ATP hydrolysis, allowing the resulting movements to be transduced through PilC to the pilins. Low-resolution cryoET images suggest that only a single ATPase fits within the socket at a time, meaning

extension and retraction ATPases must be exchanged to allow for twitching motility [43]. How the ATPases are exchanged is unknown. Recent work studying the rate of pilus extension and retraction in *P. aeruginosa* via time lapse images of live cells with labeled pili suggests a stochastic model of ATPase interactions[44]. The extension and retraction of pili did not have any discernible pattern, so it was proposed that PilB and PilT compete for interactions with PilC, however, PilU was excluded from this explanation making this model incomplete[44].

T4P ATPase motors belong to the PilT-like ATPase family [42]. PilT-like ATPases are part of the Additional Strand Catalytic 'E' (ASCE) superfamily and were previously assigned to a related AAA+ ATPase family [42,45]. PilT-like ATPases were reclassified based on their atypical Walker B (WB) motif, and unique conserved His-box and Asp-box motifs [42,46]. ATP hydrolysis in ASCE ATPases is coordinated by the Walker A (WA) and WB motifs [46,47]. The WA residues typically form a hydrogen-bonding network with the phosphate tail of ATP, while the WB motif coordinates a Mg^{2+} co-factor required for ATP hydrolysis [48,49]. In a typical WB motif, an acidic residue facilitates Mg^{2+} coordination [47]. The atypical WB motif of PilT-like ATPases lacks the acidic residue for Mg^{2+} coordination; in its place is a glycine[50]. The function of the atypical WB is unknown [42].

Other unique features of PilT-like ATPases are the Asp and His box motifs [42,46,50,51]. There are three invariant acidic residues in the Asp box; an aspartate and two glutamates [46]. PilB, PilT and PilU require the aspartate and the glutamate in the C

terminus of the Asp box for twitching motility, while only PilU needs the second glutamate for twitching motility [46]. The His box motif has two invariant histidine residues; only the second His residue is essential for twitching motility in PilB, PilT and PilU [46].

Two T4P ATPases are typically required for function, one for pilus assembly (PilB), and another for disassembly (PilT). An additional retraction ATPase, PilU, is found in many species including *Pseudomonas, Neisseria,* and *V. cholerae*. [52–54] In *P. aeruginosa*, PilB is the largest ATPase at 62 kDa, PilT is 38 kDa and PilU is an intermediate size of 42 kDa [51]. ATPase motors of the T4P system function as homohexamers. PilB and PilT are predicted to have C2 symmetry *in vivo*, however, crystal structures of PilT show multiple symmetries (C3, C6) that are not relevant to functionality when the ATPase is engaged with the motor subcomplex but are still possible [42,46,55,56]. Each interface between packing units of an ATPase can adopt an "open" (ATP accessible) or "closed" (ATP hydrolysis) conformation. PilB from *T. thermophilus* has two interfaces that are closed and four open, while PilT from *Geobacter metallireducens* and *Aquifex aeolicus* have six possible open/closed conformations [55,57].

During pilus assembly, PilB occupies the PilC-PilM socket. Hydrolysis of two ATP by PilB is predicted to cause a rotary motion of the PilB subpores that causes a corresponding 60° right-handed rotation of PilC [42]. Conformational changes in the hexamer simultaneously push PilC upwards in the IM where it "scoops" a pilin monomer

and pushes it upwards into the pilus fiber [42]. Pili are right-handed helices with 60-100° twists, which supports this model [42,58,59].

PilT occupies the PilC-PilM socket during pilus disassembly. The arrangement of the open and closed interfaces of PilT and PilB is enantiomeric, supporting their distinct roles. PilT has a conserved extension on pore loop three [42,55]. PilT hydrolysis of ATP is proposed to cause a left-handed rotation of PilC, while the pore loop pulls PilC downwards to extract a pilin from the pilus back into the membrane [42,57]. The rate of pilus disassembly is estimated to be 1000-1500 subunits/s, and retraction forces can exceed 100 pN, making PilT the most powerful biological motor known [60]. How the putative retraction ATPase PilU fits into this model is unclear. Structural data for the T4P nanomachine suggest there is no available space for PilU during PilT interactions with the motor, yet when PilU and other additional retraction ATPases are encoded in a T4P-expressing species, they are required for functional pilus dynamics.

Cellular cAMP levels are positively correlated with surface adhesion and biofilm formation in *P. aeruginosa* [17,18,61]. In *P. aeruginosa* PA14 cAMP levels increase over generations as a result of repeat Pil-Chp sensing from reversible attachment in the initial stages of biofilm formation (<20 h after surface contact). Following the initial surface contact event, each generation has higher cAMP levels than the generation before. This multigenerational memory leads to an eventual sudden increase in surface-adhered cells. Interestingly, Lee *et al.* (2018) found that *pilU* mutants of *P. aeruginosa* PA14 had

higher levels of cAMP than wild type, and took less time to establish a surface population. In contrast, *pilA, pilT,* and *pilJ* mutants had lower cAMP levels and took longer to establish a surface population. *pilU* and *pilT* mutants had opposite phenotypes, suggesting that PilU may have a unique function in regulating or responding to surface sensing.

1.4 Rationale, hypothesis, and aims

P. aeruginosa pilU mutants lose major elements of pilus functionality; they are unable to twitch even though they have retractable pili and remain susceptible to pilus-specific phages[53,62]. As observed using interferometric scattering microscopy (iSCAT), *pilU* mutants can retract pili at the same rate as their wild-type parent in liquid media but are unable to displace themselves on surfaces[62]. This is in contrast to *pilT* mutants, which are unable to retract pili and are resistant to pilus-specific phages (**Figure 3**)[62,63]. *pilU* mutants also produce more of the second messenger cAMP than *pilT* mutants and the wild type, and establish surface populations faster[61]. These data lead to the hypothesis that *pilU* contributes to the force of retraction to facilitate twitching motility, and in its absence, the increased resistance to pilus disassembly mimics surface attachment, keeping *pilU* mutants in a perpetually activated state of surface sensing. This hypothesis inspired three research aims; 1) Isolate *pilU* mutants that have regained the ability to twitch; 2) compare the force of retraction between wildtype *P. aeruginosa*

and *pilU* mutants; and 3) Investigate/ determine the mechanism for second messenger dysregulation in *pilU* mutants.

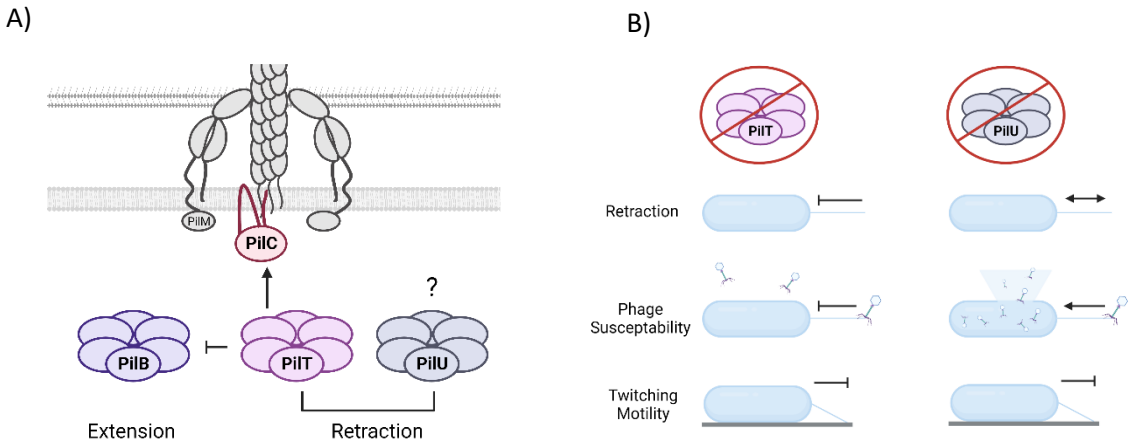

Figure 3. Schematic diagram of the motor subcomplex and phenotypic differences between retraction ATPase deletion mutants. A) The motor subcomplex, not to scale. PilT can occupy the PilC-PilM socket when PilB is absent, but where and how PilU interacts with this system is unknown. B) *pilU* mutants are able to retract their pili, while *pilT* mutants are not, leading to different phenotypes.

Aim 1: Isolate pilU mutants that have regained the ability to twitch

Mutagenesis studies can be used to determine the function of specific genes and their protein products by either assessing knockout phenotypes or isolating mutants that restore function in a knockout background. For the latter, mutations that restore function can identify interaction partners of the protein in question or provide an indicator of a protein's role in a larger system. A recent publication by Chlebek et al. (2021) found mutations in the major competence pilin gene of *Vibrio cholerae* that restored competence (free DNA uptake) in a retraction ATPase deficient background[64].

Here we hypothesized that it would be possible to isolate "gain-of-twitching" mutants in *pilU::*Tn5 and *ΔpilU* backgrounds. Determining how such mutations affected the T4P system would provide insight into PilU's role.

Aim 2: Compare the force of retraction between wild-type P. aeruginosa and pilU mutants

P. aeruginosa pilU mutants are phage susceptible but are incapable of twitching motility. The pili are retracted but without PilU, the bacteria cannot displace themselves, suggesting a significant decrease in force generation during retraction. Here we aim to use a polyacrylamide micropillar assay (PoMP) to measure the force of retraction in a *ΔpilU* background and compare it to that of wild-type *P. aeruginosa*.

Aim 3: Investigate/ determine the mechanism for second messenger dysregulation in pilU mutants

pilU mutants have increased levels of the second messenger cAMP, which causes a signal cascade resulting in the production of exopolysaccharides used for surface adhesion[61]. The colony morphology of *pilU* mutants is also strikingly different from the wild type, *pilU* mutants grow in small rugose puncta on solid media while their wild-type parent grows as large glossy colonies, further adding evidence that *pilU* mutants have an unusual exopolysaccharide matrix. The second half of this hypothesis supposes that second messenger and subsequent exopolysaccharide dysregulation in *pilU* mutants is a result of altered tension while retracting pili. The first aim which proposes to search for

mutants where the presence of PilU and twitching motility are uncoupled, will also result in the generation of strains where it is possible to distinguish the relative contributions of pilus retraction versus PilU to surface sensing. These strains can be used to answer how PilU contributes to second messenger regulation.

CHAPTER 2. MATERIAL AND EXPERIMENTAL PROCEDURES

2.1 Bacterial strains and plasmids

Bacterial strains and plasmids used for this project are summarized in **Table 1** and **Table 2**. Bacterial strains were grown at 37°C overnight in Luria-Bertani (LB) or LB 1.5% agar unless otherwise specified. For *P. aeruginosa* strains carrying plasmids with a gentamicin (Gm) resistant cassette 30 µg mL^{-1} was added to the media, for *E. coli* strains 15 µg mL^{-1} was added. For strains carrying the arabinose inducible vector pBADGr, L-arabinose was added to media in a gradient of concentrations: 0.02%, 0.05%, 0.1% and 0.2%. Plasmid constructs were initially introduced into chemically-competent *E. coli* DH5α by heat shock. Verified constructs were introduced to *E. coli* SM10 and/or *P. aeruginosa* by electroporation.

Plasmid constructs were made using standard cloning techniques and the restriction enzymes listed in **Table 3**. Deletion constructs were built by cloning 500 bp up- and downstream of the corresponding gene plus a complementary region of 20 bp between both up- and down stream fragments to allow for overlap extension PCR. The

products were then ligated to pEX18Gm to build the complete construct. Knock-in constructs were built by the same technique with the up- and downstream regions flanking the point mutation, and the point mutation introduced in the complementary regions of the primers. Deletion and knock-in mutation constructs were introduced into *E. coli* SM10 and conjugated into the PAO1 parent strain by standard methods previously described[65]. The mutations were confirmed with PCR and Sanger sequencing (Mobix, McMaster Genomics Facility, Hamilton).

Table 1. Bacterial strains used in this study

Strain	Characteristics	Source
E. coli strains		
E. coli DH5α	F- *φ80lacZΔM15 Δ(lacZYA-argF)U169 recA1 endA1 hsdR17(rk-, mk+) phoA supE44 thi-1 gyrA96 relA1 λ*	Invitrogen
E. coli SM10	*thi-1 thr leu tonA lacY supE recA::RP4-2- Tc::Mu* (KmR)	(66)
P. aeruginosa strains		
mPAO1 WT	WT	(67)
mPAO1 WT + pUCP20Gm	WT with pUCP20Gm	Burrows lab
mPAO1 WT + pUCP20Gm-*pilU*	WT with pUCP20Gm containing *pilU*	(This work)
mPAO1 WT + pBADGr	WT with pBADGr	Burrows lab
mPAO1 WT + pBADGr-*pilA*	WT with pBADGr containing *pilA*	Burrows lab
mPAO1 *ΔpilU*	Chromosomal deletion of *pilU*	(This work)
mPAO1 *ΔpilU* + pUCP20Gm	Chromosomal deletion of *pilU* with pUCP20Gm	(This work)
mPAO1 *ΔpilU* + pUCP20Gm-*pilU*	Chromosomal deletion of *pilU* with pUCP20Gm containing *pilU*	(This work)

mPAO1 *ΔpilU* + pBADGr	Chromosomal deletion of *pilU* with pBADGr	(This work)
mPAO1 *ΔpilU* + pBADGr-*pilA*	Chromosomal deletion of *pilU* with pBADGr containing *pilA*	(This work)
mPAO1 *ΔpilU* 2mut19c1	EMS mutated twitching isolate of a chromosomal deletion of *pilU*	(This work)
mPAO1 *ΔpilU* 2mut22c1	EMS mutated twitching isolate of a chromosomal deletion of *pilU*	(This work)
mPAO1 *ΔpilU* 2mut24c1	EMS mutated twitching isolate of a chromosomal deletion of *pilU*	(This work)
mPAO1 *ΔpilU* 2mut31c2	EMS mutated twitching isolate of a chromosomal deletion of *pilU*	(This work)
mPAO1 *ΔpilU* 2mut34c1	EMS mutated twitching isolate of a chromosomal deletion of *pilU*	(This work)
mPAO1 *ΔpilU* 2mut48c2	EMS mutated twitching isolate of a chromosomal deletion of *pilU*	(This work)
mPAO1 *ΔpilU* 2mut51c1	EMS mutated twitching isolate of a chromosomal deletion of *pilU*	(This work)
mPAO1 *ΔpilU* 2mut53c1	EMS mutated twitching isolate of a chromosomal deletion of *pilU*	(This work)
mPAO1 *ΔpilU* 2mut58c1	EMS mutated twitching isolate of a chromosomal deletion of *pilU*	(This work)
mPAO1 *ΔpilU* 2mut58c2	EMS mutated twitching isolate of a chromosomal deletion of *pilU*	(This work)
mPAO1 *ΔpilU* 2mut70c1	EMS mutated twitching isolate of a chromosomal deletion of *pilU*	(This work)
mPAO1 *ΔpilU* 2mut71c1	EMS mutated twitching isolate of a chromosomal deletion of *pilU*	(This work)
mPAO1 *ΔpilU* PilA M13I	Chromosomal deletion of *pilU* and a chromosomal substitution of PilA M13 to isoleucine	(This work)
mPAO1 *ΔpilU* PilA P28L	Chromosomal deletion of *pilU* and a chromosomal substitution of PilA P28 to leucine	(This work)
mPAO1 *ΔpilU* PilA V34F	Chromosomal deletion of *pilU* and a chromosomal substitution of PilA V34 to phenylalanine	(This work)
mPAO1 *ΔpilU* PilA A40T	Chromosomal deletion of *pilU* and a chromosomal substitution of PilA A40 to threonine	(This work)

mPAO1 *ΔpilU* PilA P48L	Chromosomal deletion of *pilU* and a chromosomal substitution of PilA P48 to leucine	(This work)
mPAO1 *ΔpilU* PilA G60R	Chromosomal deletion of *pilU* and a chromosomal substitution of PilA G60 to arginine	(This work)
mPAO1 *ΔpilU* PilA G130E	Chromosomal deletion of *pilU* and a chromosomal substitution of PilA G130 to glutamate	(This work)
mPAO1 *ΔpilU* PilA M13I + pUCP20Gm	Chromosomal deletion of *pilU* and a chromosomal substitution of PilA M13 to isoleucine with pUCP20Gm	(This work)
mPAO1 *ΔpilU* PilA P28L + pUCP20Gm	Chromosomal deletion of *pilU* and a chromosomal substitution of PilA P28 to leucine with pUCP20Gm	(This work)
mPAO1 *ΔpilU* PilA V34F + pUCP20Gm	Chromosomal deletion of *pilU* and a chromosomal substitution of PilA V34 to phenylalanine with pUCP20Gm	(This work)
mPAO1 *ΔpilU* PilA A40T + pUCP20Gm	Chromosomal deletion of *pilU* and a chromosomal substitution of PilA A40 to threonine with pUCP20Gm	(This work)
mPAO1 *ΔpilU* PilA P48L + pUCP20Gm	Chromosomal deletion of *pilU* and a chromosomal substitution of PilA P48 to leucine with pUCP20Gm	(This work)
mPAO1 *ΔpilU* PilA G60R + pUCP20Gm	Chromosomal deletion of *pilU* and a chromosomal substitution of PilA G60 to arginine with pUCP20Gm	(This work)
mPAO1 *ΔpilU* PilA G130E + pUCP20Gm	Chromosomal deletion of *pilU* and a chromosomal substitution of PilA G130 to glutamate with pUCP20Gm	(This work)
mPAO1 PilA *ΔpilU* M13I + pUCP20Gm-*pilU*	Chromosomal deletion of *pilU* and a chromosomal substitution of PilA M13 to isoleucine with pUCP20Gm containing *pilU*	(This work)
mPAO1 *ΔpilU* PilA P28L + pUCP20Gm-*pilU*	Chromosomal deletion of *pilU* and a chromosomal substitution of PilA P28 to leucine with pUCP20Gm containing *pilU*	(This work)
mPAO1 *ΔpilU* PilA V34F + pUCP20Gm-*pilU*	Chromosomal deletion of *pilU* and a chromosomal substitution of PilA	(This work)

	V34 to phenylalanine with pUCP20Gm containing *pilU*	
mPAO1 *ΔpilU* PilA A40T + pUCP20Gm-*pilU*	Chromosomal deletion of *pilU* and a chromosomal substitution of PilA A40 to threonine with pUCP20Gm containing *pilU*	(This work)
mPAO1 *ΔpilU* PilA P48L + pUCP20Gm-*pilU*	Chromosomal deletion of *pilU* and a chromosomal substitution of PilA P48 to leucine with pUCP20Gm containing *pilU*	(This work)
mPAO1 *ΔpilU* PilA G60R + pUCP20Gm-*pilU*	Chromosomal deletion of *pilU* and a chromosomal substitution of PilA G60 to arginine with pUCP20Gm containing *pilU*	(This work)
mPAO1 *ΔpilU* PilA G130E + pUCP20Gm-*pilU*	Chromosomal deletion of *pilU* and a chromosomal substitution of PilA G130 to glutamate with pUCP20Gm containing *pilU*	(This work)
mPAO1 *ΔpilU* PilA M13I + pBADGr	Chromosomal deletion of *pilU* and a chromosomal substitution of PilA M13 to isoleucine with pBADGr	(This work)
mPAO1 *ΔpilU* PilA P28L + pBADGr	Chromosomal deletion of *pilU* and a chromosomal substitution of PilA P28 to leucine with pBADGr	(This work)
mPAO1 *ΔpilU* PilA V34F + pBADGr	Chromosomal deletion of *pilU* and a chromosomal substitution of PilA V34 to phenylalanine with pBADGr	(This work)
mPAO1 *ΔpilU* PilA A40T + pBADGr	Chromosomal deletion of *pilU* and a chromosomal substitution of PilA A40 to threonine with pBADGr	(This work)
mPAO1 *ΔpilU* PilA P48L + pBADGr	Chromosomal deletion of *pilU* and a chromosomal substitution of PilA P48 to leucine with pBADGr	(This work)
mPAO1 *ΔpilU* PilA G60R + pBADGr	Chromosomal deletion of *pilU* and a chromosomal substitution of PilA G60 to arginine with pBADGr	(This work)
mPAO1 *ΔpilU* PilA G130E + pBADGr	Chromosomal deletion of *pilU* and a chromosomal substitution of PilA G130 to glutamate with pBADGr	(This work)
mPAO1 *ΔpilU* PilA M13I + pBADGr-*pilA*	Chromosomal deletion of *pilU* and a chromosomal substitution of PilA	(This work)

	M13 to isoleucine with pBADGr containing *pilA*	
mPAO1 *ΔpilU* PilA P28L + pBADGr-*pilA*	Chromosomal deletion of *pilU* and a chromosomal substitution of PilA P28 to leucine with pBADGr containing *pilA*	(This work)
mPAO1 *ΔpilU* PilA V34F + pBADGr-*pilA*	Chromosomal deletion of *pilU* and a chromosomal substitution of PilA V34 to phenylalanine with pBADGr containing *pilA*	(This work)
mPAO1 *ΔpilU* PilA A40T + pBADGr-*pilA*	Chromosomal deletion of *pilU* and a chromosomal substitution of PilA A40 to threonine with pBADGr containing *pilA*	(This work)
mPAO1 *ΔpilU* PilA P48L + pBADGr-*pilA*	Chromosomal deletion of *pilU* and a chromosomal substitution of PilA P48 to leucine with pBADGr containing *pilA*	(This work)
mPAO1 *ΔpilU* PilA G60R + pBADGr-*pilA*	Chromosomal deletion of *pilU* and a chromosomal substitution of PilA G60 to arginine with pBADGr containing *pilA*	(This work)
mPAO1 *ΔpilU* PilA G130E + pBADGr-*pilA*	Chromosomal deletion of *pilU* and a chromosomal substitution of PilA G130 to glutamate with pBADGr containing *pilA*	(This work)
mPAO1 *ΔfliC*	Chromosomal deletion of *fliC*	Burrows lab
mPAO1 *ΔpilUΔfliC*	Chromosomal deletion of *pilU* and *fliC*	(This work)
mPAO1 *ΔpilTΔfliC*	Chromsomal deletion of *pilT* and *fliC*	(This work)
mPAO1 *ΔpilCΔfliC*	Chromosomal deletion of *pilC* and *fliC*	(This work)
PA0396	*pilU::*Tn5 mutant, Tn5 B21 insertion in *pilU*	(68)
PA0396 1mut2c1	EMS mutated twitching isolate of a *pilU::*Tn5 mutant	(This work)
PA0396 1mut4c	EMS mutated twitching isolate of a *pilU::*Tn5 mutant	(This work)
PA0396 1mut7c1	EMS mutated twitching isolate of a *pilU::*Tn5 mutant	(This work)

mPAO1 *ΔpilT*	Chromsomal deletion of *pilT*	(This work)
mPAO1 *ΔpilTΔpilU*	Chromsomal deletion of *pilT* and *pilU*	(This work)
mPAO1 *ΔpilTΔpilU* $pilA_{A40T}$	Chromsomal deletion of *pilT*, *pilU* and a chromosomal substitution of PilA α-helical residue A40 to threonine	(This work)
mPAO1 *ΔpilU* $pilY1_{S59G}$	Chromosomal deletion of *pilU* and a chromosomal substitution of PilY1 residue S59 to glycine	(This work)
mPAO1 *ΔpilU* $pilY1_{G1120D}$	Chromosomal deletion of *pilU* and a chromosomal substitution of PilY1 residue G1120 to asparagine	(This work)
mPAO1 *ΔsadC* + pBADGr-*sadC*	Chromosomal deletion of *sadC* with pBADGr containing *sadC*	(14)

Table 2. Plasmids used in this study

Vector	Characteristics	Source
pEX18Gm	Suicide vector used for gene replacement	(30)
pUCP20Gm	Shuttle vector with SmaI-flanked Gm cassette inserted into ScaI site in *bla*	(69)
pBADGr	Broad host range arabinose inducible vector used for complementation; ori araC-PBAD Gmr mob+	(70)
pEX18Gm-*ΔpilU*	pEX18Gm with a *pilU* deletion construct	(This work)
pEX18Gm-*ΔpilT*	pEX18Gm with a *pilT* deletion construct	Burrows lab, unpublished
pEX18Gm-*ΔpilC*	pEX18Gm with a *pilC* deletion construct	(This work)
pEX18Gm-*ΔfliC*	pEX18Gm with a *fliC* deletion construct	Burrows lab
pEX18Gm-*ΔpilTΔpilU*	pEX18Gm with a *pilT* deletion construct for use in a *ΔpilU* background	(This work)
pEX18Gm-*pilA* M13I	pEX18Gm with a knockin construct for a substitution of PilA M13 to isoleucine	(This work)
pEX18Gm-*pilA* P28L	pEX18Gm with a knockin construct for a substitution of PilA P28 to leucine	(This work)
pEX18Gm-*pilA* V34F	pEX18Gm with a knockin construct for a substitution of PilA V34 to phenylalanine	(This work)
pEX18Gm-*pilA* A40T	pEX18Gm with a knockin construct for a substitution of PilA A40 to threonine	(This work)

pEX18Gm-*pilA* P48L	pEX18Gm with a knockin construct for a substitution of PilA P48 to leucine	(This work)
pEX18Gm-*pilA* G60R	pEX18Gm with a knockin construct for a substitution of PilA G60 to arginine	(This work)
pEX18Gm-*pilA* G130E	pEX18Gm with a knockin construct for a substitution of PilA G130 to glutamate	(This work)
pUCP20Gm-*pilU*	pUCP20Gm expressing *pilU*	(This work)
pBADGr-*pilA*	pBADGr expressing *pilA*	Burrows lab
pBADGr-*sadC*	pBADGr expressing *sadC*	(14)

Table 3. Primers used in this study [a,b].

Primer Name	Sequence (5'→3')
pilU F	ATTAGGTACCATCATGGAATTCGAAAAGC
pilU R	ATTACTGCAGTCAGCGGAAGCGCCGGCCG
pilA seq F	CCCTCTGAACGAATCGCAGG
pilA seq R	GCTGCCAAATCGAGGAAATCC
pilU F1	ATTAGAGCTCAATCGGTGATCTCGCAGACC
pilU F2	AACTCGAGCCGCAAGCATGCTGAACTGAGCCTGGAAATCACCGA
pilU R1	TTCAGCATGCTTGCGGCTCGAGTTGGAGCCGCCCTTTTCCAC
pilU R2	ATTAAAGCTTGCAACAGCCTGAACGTCAAG
pilC F1	ATTCGAGCTCATCCGCCAGGTACGCAATGG
pilC R1	GGTCGGTACCCTTCGTTCTGCGAGTCTTCC
pilC F2	CGCTGGTACCCTACATCCAGGGCTACTACC
pilC R2	GGATAAGCTTCGCCTGGGTTACAAGACCGC
pilTpilU F1	ATTAGAGCTCGTTCAAGGGCAGGTCGGCCA
pilTpilU R1	GGGCGTTCTCGCGGCTGATGGTCCGAAGCGCCCTGTTTG
pilTpilU F2	CAAACAGGGCGCTTCGGACCATCAGCCGCGAGAACGCCC
pilTpilU R2	ATTAAAGCTTGGTCGATCACCAGCGGCAAG
pilA M13I F1	ATTAGAGCTCCCATTAGAGGAACCCAATCA
pilA M13I R1	CGAACTGAT**A**ATCGTGGTTG
pilA M13I F2	CAACCACGAT**T**ATCAGTTCG
pilA M13I/P28L R2	ATTAAAGCTTGCTATTCAGGTCGCAATAGG
pilA P28L/V34F F1	ATTAGAGCTCCCTCTGAACGAATCGCAGG
pilA P28L R1	ATTGCCATTC**T**CCAGTATCAG
pilA P28L F2	CTGATACTGG**A**GAATGGCAAT
pilA V34F R1	CAGAACTAT**T**TTGCGCGTTCG
pilA V34F F2	CGAACGCGCAA**A**ATAGTTCTG

pilA V34F R2	ATTAAAGCTTGCTATTCAGGTCGCAATAGGC
pilA A40T F1	ATTAGAGCTCCATGCGCCTCACCCTCTGA
pilA A40T R1	GTTCGGAAGGT**A**CTTCGGCG
pilA A40T F2	CGCCGAAG**T**ACCTTCCGAAC
pilA A40T R2	ATTAAAGCTTCGAACTGCTCGGCGGACA
pilA P48L/G60R F1	ATTAGAGCTCCTACATCTCCATCGGCACC
pilA P48L R1	CGATCAACC**T**GCTGAAGACC
pilA P48L F2	GGTCTTCAGC**A**GGTTGATCG
pilA P48L/G60R R2	ATTAAAGCTTCACCAGCGACAGCTTGTTG
pilA G60R R1	GCTGTCGCGT**A**GAATTGCTG
pilA G60R F2	CAGCAATTC**T**ACGCGACAGC
pilA G130E F1	ATTAGAGCTCGCATAGCACCCGGCAAGCC
pilA G130E R1	TGCGGATG**A**GGTCTGGGCTT
pilA G130E F2	AAGCCCAGACC**T**CATCCGCA
pilA G130E/N87K R2	ATTAAAGCTTGGACAGGCCGCTCAGTTGG

[a]-Restriction sites are underlined

[b]-Mismatched bases for site directed mutagenesis are bolded

2.2 Twitching motility assay

Single colonies from an LB 1.5% culture were stab-inoculated with a micropipette tip in 1% LB agar to the agar-plastic interface of cell culture-treated plates (OmniTray Cell Culture Treated, Thermo Fisher Scientific)[63]. Plates were incubated for 12 h at 37°C. Following incubation, the agar was removed, and the plates were stained with 1% crystal violet for 10-15 min before washing with diH_2O. Plates were imaged using a flatbed scanner and twitching zones were measured using ImageJ (http://imagej.nih.gov/ij/, NIH, Bethesda, MD)[63].

2.3 Ethyl methane sulfonate mutagenesis experiments

Gain-of-function mutants were generated using a modified chemical mutagenesis protocol based on Snyman et al. (2021), Andreoni et al. (1995) Govan et al. (1978) and Montie et al. (1982) [71–74]. Briefly, *P. aeruginosa* PAO1 *pilU::*Tn5 and *ΔpilU* were grown in 5 mL LB at 37°C shaking at 200 rpm overnight. One hundred microlitres of the overnight culture was used to inoculate 5 mL LB and strains were grown in the same conditions to an OD_{600} between 0.4-0.6. Ethyl methane sulfonate (EMS) was then added to the cultures to final concentrations of 200, 100, 50, 20, 10, 5 or 0 µg/mL, then the cultures were vortexed for 30 s before being incubated at 37°C without shaking for 1 h. One mL of each culture was centrifuged at 16 000 *x g* for 1 min and the supernatant was discarded. The cell pellet was resuspended in 1 mL 10 mM KPO_4 pH 7 and centrifuged at 16 000 *x g* for 1 min; this step was repeated a second time. Following washing with 10 mM KPO_4 the pellet was resuspended in 1 mL LB. Ten microlitre aliquots were spotted on LB 1.5% agar plates. The plates were incubated for 24 h at 37°C, and MIC was estimated at the concentration where growth was inhibited. EMS mutagenesis was repeated at the estimated MIC of 50 µg/mL for the *pilU::*Tn5 strain and at the lowest concentration of 5 µg/mL for the *ΔpilU* strain. These plates were incubated on the bench for 5 days at room temperature. Motile flares that emerged from the site of inoculation were selected, used to stab inoculate a 1% LB agar twitching assay plate and incubated at 37°C overnight. After the agar was removed, twitching colonies were scraped from the bottom of the plate and streaked to single colonies on LB 1.5% agar. Single colonies were assessed for twitching a second time before preparation of LB 15% -80°C glycerol

stocks. We determined that 5 µM EMS was sufficient to reliably induce gain-of-twitching mutations. Five µM EMS was then used to repeat this experiment for PAO1 *ΔpilU*. Whole genomic DNA (Wizard®Genomic DNA Purification Kit) from gain of twitching isolates from the 5 µM EMS PAO1 *ΔpilU* and 50-5µM EMS PAO1 *pilU::*Tn5 experiments with their respective parent strains were sent for whole genome sequencing at Seqcenter (Pittsburgh, PA) then compared to their respective parent strains for mutations using Breseq[75].

2.4 Phage sensitivity assay

P. aeruginosa strains to be tested were subcultured at 37°C shaking at 200 rpm in LB until reaching OD_{600} 0.2-0.3. Cultures were standardized to OD_{600} 0.2 before spot inoculating on LB 1.5% agar plates in 6 µL aliquots. The aliquots were dried then 4 µL aliquots of PO4 phage were added on top of each spot, beginning at a concentration of 10^8 PFU per mL progressing to 10^1. The plates were incubated at 37°C for 24 h before imaging[76]. This assay has one biological replicate in a set of three technical replicates.

2.5 Sheared surface protein assays

Sheared surface protein assays were done as described previously [77,78] . Strains were grown from -80°C freezer stock son 1.5% LB agar at 37°C overnight before streaking in a 5x5 grid pattern on another 1.5% LB agar plate and incubating in the same conditions overnight. Cells were scraped from the plate and resuspended in 3 mL 1X PBS (pH 7.3), then vortexed for 15 s (x2) before transferring to Eppendorf tubes and

centrifuging for 30 min at 16 000 *x g*. The supernatant was transferred to a new tube and incubated in 10% 1 M $MgCl_2$ overnight at 4°C. The supernatant was then centrifuged at 16 000 *x g* for 30 min, the supernatant was discarded, the resulting pellet was re-centrifuged at 16 000 *x g* for 1 min, and remaining supernatant was removed by pipetting. The pellet was resuspended in 50 µL 1X SDS loading buffer and boiled for 10 min. Surface shearing assay products were stored at -20°C before use.

2.6 SDS-PAGE and Western blotting

Surface sheared protein assays or cell pellets from 1 ml of culture at OD_{600} 0.6 were resuspended in 50 µL of 1X SDS-PAGE sample buffer and boiled for 10 min. SDS-PAGE samples were centrifuged at 16 000 *x g* for 1 min before loading into a 15% acrylamide SDS-PAGE gel. Proteins were separated at 80V for 1 h. Gels were stained with Coomassie brilliant blue 1.2 mg/mL for 1 h then destained overnight. Gels for Western blots were transferred to a nitrocellulose membrane at 225 mA for 1 h. The membrane was blocked overnight with 1X PBS 5% skimmed milk at 4°C before incubating overnight with 1/5000 dilution of primary antibody in 1X PBS at room temperature shaking at 200 rpm[79]. Unbound primary antibody was washed off with 1X PBS for 10 min at 200 rpm (x4) before incubating with secondary antibody at a 1/2500 dilution for 1hr[79]. The blot was resolved with 0.25g/mL NBT and 0.1% BCIP in 1X PBS before imaging[79].

2.7 Colony surface phenotypes

To evaluate this phenotype in gain-of-function mutants, single colonies from an overnight LB 1.5% agar culture were streaked out in individual sections of a LB 1.5% agar plate and incubated overnight at 37°C before imaging on a standard scanner.

2.8 Congo Red binding assay

Single colonies from overnight LB 1.5% agar cultures of the strains of interest were used to inoculate 3 ml LB cultures which were incubated at 37°C overnight with 200 rpm shaking. One mL of the overnight cultures were aliquoted into Eppendorf tubes and centrifuged at 16 000 *x g* to pellet cells. The supernatant was removed and cell pellets were washed with 1X PBS twice before making a 100-fold dilution in 100 µL 1X PBS and spotting 5 µL on tryptic soy broth 1.5% agar containing 40 µg/mL Congo red and 15 µg/mL Coomassie brilliant blue[80]. Plates were incubated at 25°C for 5 days before imaging with an Azure biosystems imager set to true colour imaging.

2.9 Polyacrylamide micropillar assay

Micropillars were cast on an activated glass cover slip using a microfabricated silicon mold with evenly spaced holes[81]. Twenty µL of 20% and 0.2% polyacrylamide gel was aliquoted onto the mold. The mold was removed in 50 mM HEPES pH 7.3 after 15 min of curing. The micropillar surface was activated by incubating in 0.4% sulfo-SANPAH HEPES pH 7.3 under a UV light for 5 min, repeating the process twice. The micropillars were coated with Poly-L-Lysine by aliquoting 400 µL onto the micropillar surface and incubating at 37°C for 1 h. Polyacrylamide concentrations of 20% and 0.2% were used for

this study. The stiffness constant of the pillars was 250 pN/µm and 25 pN/µm respectively, as measured by optical magnetic tweezers.

CHAPTER 3. RESULTS

3.1 Gain-of-twitching mutations in *ΔpilU* and *pilU::Tn5* backgrounds

Many twitching species encode PilT, but lack PilU homologues. However, both PilU and PilT are required for twitching motility in *P. aeruginosa*. *P. aeruginosa pilU* mutants can retract pili to some extent, as seen directly with iSCAT imaging of cells in liquid, and indirectly via susceptibility to pilus-specific phages [62,63]. Compared to wild type or *ΔpilT* mutants, *ΔpilU* mutants establish surface populations more rapidly and have increased levels of intracellular cAMP, behaving as if they are already surface engaged [61]. Therefore, it is possible that PilU enhances the force of retraction generated by PilT when pili are tethered to a surface, and that in its absence, the inability to retract tethered pili amplifies surface sensing responses. To understand what PilU might be doing in the T4P system we selected for twitching gain-of-function mutants in *pilU::*Tn5 and *ΔpilU* backgrounds. A series of ethyl methanesulfonate (EMS) chemical mutagenesis experiments were conducted to generate mutants in which twitching was restored in the absence of PilU.

EMS induces heritable G:C to A:T transitions by alkylating guanine, forming O^6 ethylguanine, which mis-pairs with thymine during DNA repair and replication[82] (**Supplementary Figure 1**). The initial concentration of EMS used was selected by

determination of the minimum inhibitory concentration (MIC) of EMS for *P. aeruginosa*. As *P. aeruginosa* was unable to grow at concentrations above 50 µM EMS, this concentration was used in the first set of mutagenesis experiments with a *pilU::*Tn5 mutant strain. EMS was added to the liquid culture during the log phase of growth (OD_{600} 0.4-0.6) before aliquoting 10 µL spots on agar plates. The plates were incubated at room temperature for 5 days, when irregular rough edges and small round glossy edges were observed breaking away from the point of inoculation (**Figure 4**). These emergent sectors were selected for twitching assays. Interestingly, none of colonies with the rough irregular phenotypes twitched, suggesting that some other form of motility was being used. Two independent mutagenesis experiments resulted in the isolation of 24 gain-of-function twitching mutants. Twitching zones of separate colonies were difficult to distinguish, but an estimated 20% of inoculation points for *pilU::*Tn5 had a twitching zone. The twitching zones between *ΔpilU* spots were easier to distinguish, and 12% had twitching zones. No reproducible twitching edges were observed for *pilU::*Tn5 and *ΔpilU* strains in the absence of exposure to EMS.

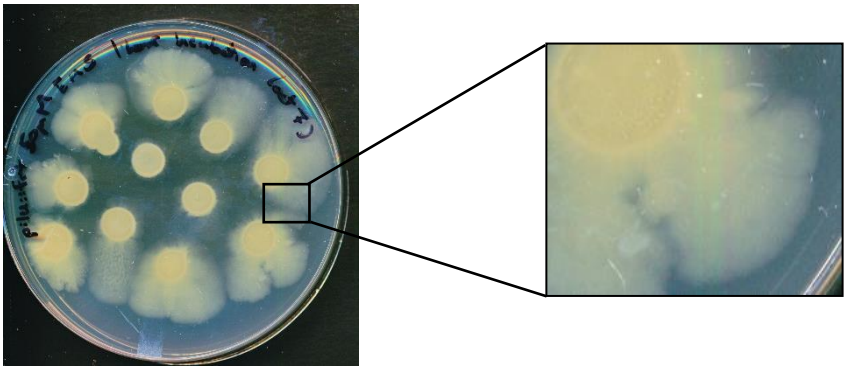

Figure 4. Original EMS mutagenesis agar plate. *P. aeruginosa* PAO1 *pilU*::Tn5 exposed to 50 µM EMS and plated on LB 1.5% agar for five days incubated at room temperature. Escape mutants can be seen spreading from the point of inoculation.

Following the initial round of experimentation, we used a lower concentration of EMS to reduce the potential for multiple mutations, which could complicate subsequent analyses. The lowest concentration at which mutations resulting in changes in colony morphology were observed was 5 µM EMS (**Figure 5**). In addition, we switched to a *ΔpilU* mutant background instead of a *pilU::*Tn5 mutant to prevent restoration of *pilU* expression. From this new round of mutagenesis, 15 twitching mutants were isolated. Twitching motility and growth rates of the *ΔpilU* and *pilU::*Tn5 mutants were compared to that of wild-type PAO1 (**Figure 4**). None of the mutants had growth defects (**Supplementary Figure 1**).

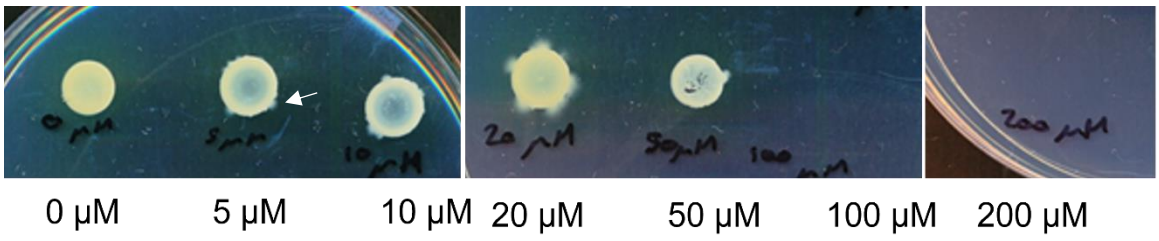

Figure 5. Estimation of EMS MIC. *P. aeruginosa* PAO1 *ΔpilU* exposed to increasing concentrations of EMS for 24 h at 37°C and 200 rpm shaking then spotted on LB 1.5% agar and incubated overnight at 37°C. The white arrow points to one of the "break away" edges described.

Table 4. Summary of mutations found in *ΔpilU and pilU::*Tn5 gain-of-twitching mutants[a].

ΔpilU mutant	Mutations	*pilU::*Tn5 mutant	Mutations
2mut19c1	PilA^{G60R}, PA1036^{V77V}	1mut2c1	PilY1^{S59G}, PknD^{A188A}, RplI^{A63T}, PA2735^{R647R}
2mut22c1	PilA^{G130E}, BkdB$^{P143\ fs}$		
2mut24c1	PilA^{P48L}		
2mut31c2	PilA^{M13I}, BkdB$^{P143\ fs}$, FptA^{R573H}	1mut4c1	PilY1^{A219T},PilY1^{G1120D}, DecR^{A89A}, SecA^{P529L}, OxyR1 (intergenic), IlvI (intergenic), PA4621^{V130V}, CdrA^{R113R}, PssA^{A155V}
2mut34c1	PilA^{P28L}, BkdB$^{P143\ fs}$		
2mut48c2	PilA^{V34F}, BkdB$^{P143\ fs}$		
2mut51c1	PilA^{A40T}, BkdB$^{P143\ fs}$		
2mut53c1	PilA^{N87K}		
2mut58c1	PilA^{G60R}	1mut7c1	PilY1^{G1120D}, BepF^{L330F}, PA0725^{S5F}
2mut58c2	PilC^{V80E}, BkdB$^{P143\ fs}$		
2mut71c1	PilA^{N87K}, MurE^{R367C}, ArgJ^{G105A}		

[a]-Frame shifts are denoted by "fs"

PilU expression in the *pilU::*Tn5 gain-of-function mutants was tested by Western blot of whole cell lysate using anti-PilU sera. Two mutants expressed PilU and were excluded from further follow up. Lack of the *pilU* gene in the gain-of-function *ΔpilU* mutants was verified using PCR and sequencing. Then, genomic DNA from select mutants was sequenced followed by identification of genetic differences between parent and mutant strains using BreSeq [75]. The mutations are summarized in **Table 4**.

Twitching motility of the mutants compared to a wild-type control was quantified (**Figure 6**). In the *ΔpilU* background, only 2mut51c1 twitched similar to wild type; all others were ≥ 60% of wild type. For the *pilU::*Tn5 mutants, 1mut4c1 and 1mut7c1 had

twitching 61.7% ± 9.1 and 69.3% ± 7.7 to wildtype respectively. Mutant 1mut2c1 twitched substantially less, at 12.3% ± 7.3.

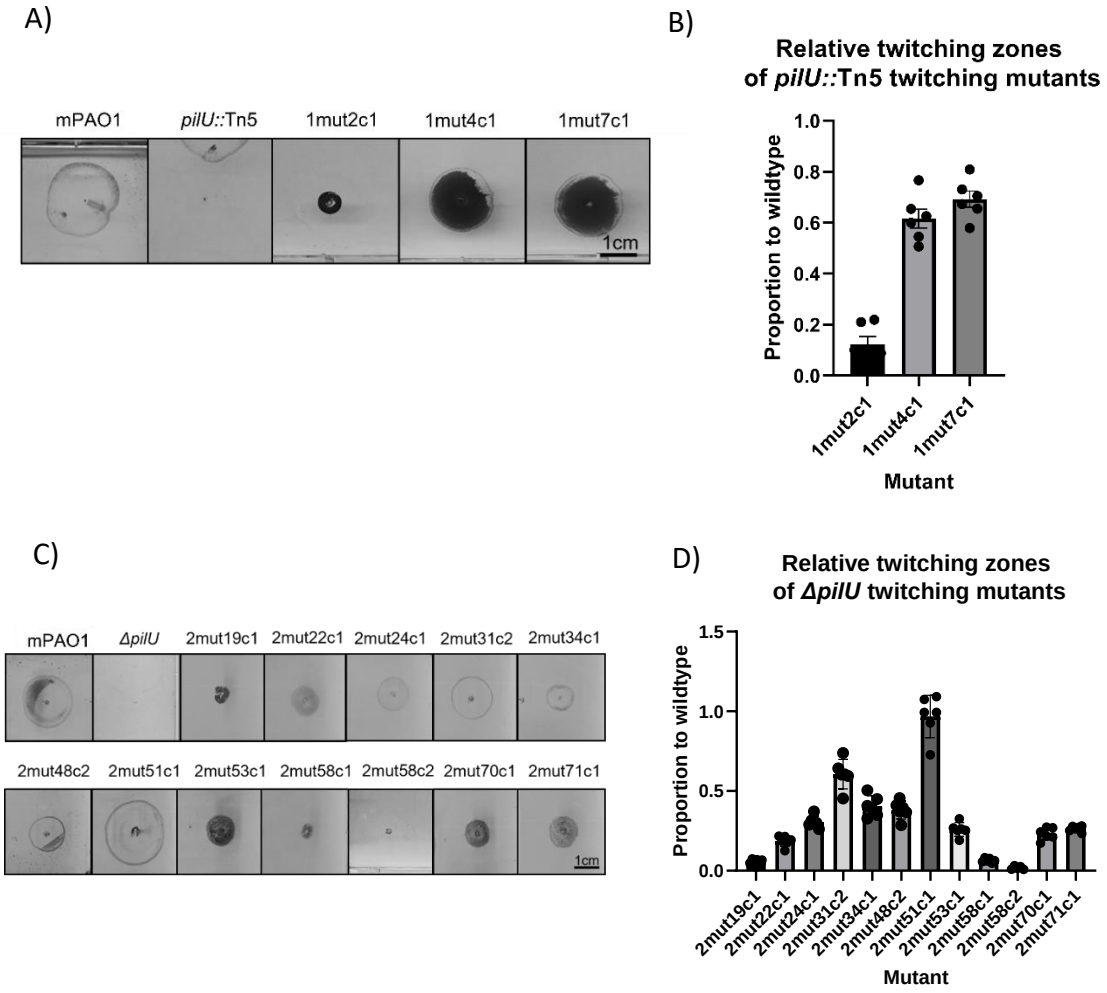

Figure 6. Twitching motility in gain-of-function mutants. A) Representative twitching zones of gain-of-twitching mutants compared to wild-type *P. aeruginosa* and the *pilU::*Tn5 parent strain B) Quantification of *pilU::*Tn5 gain-of-twitching mutant twitching zones compared to wild type *P. aeruginosa* PAO1. C) Representative twitching zones of gain-of-twitching mutants compared to wildtype *P. aeruginosa* and the *ΔpilU* parent strain. D) Quantification of *ΔpilU* gain-of-twitching mutant twitching zones compared to wild type *P. aeruginosa* PAO1.. N = 2 biological replicates each with 3 technical replicates for all panels.

No mutations were shared between the *pilU::*Tn5 and *ΔpilU* gain-of-twitching mutants. In the *pilU::*Tn5 group, multiple mutations in *pilY1* – encoding the putative adhesin component of the pilus tip complex – were identified, while all other mutations appeared in only one isolate (**Table 4**). These mutations include $pilY1_{S59G}$, $pilY1_{A219T}$, and $pilY1_{G1120D}$ that occurred twice. Mutant 1mut4c1 had two mutations in *pilY1*, $pilY1_{A219T}$ and $pilY1_{G1120D}$. The vWA-like domain of PilY1 is located in the N-terminus between residues 48-368 adjacent the Sec secretion signal (residues 1-32) that allows its transportation across the IM [83,84]. $pilY1_{S59G}$ lies at the beginning of the vWA domain. The C-terminal region of PilY1 (residues 585-997) shares 24% identity and 46% similarity with the *Neisseria* pilus adhesin PilC1 (a PilY1 homologue) that is required for twitching motility[83,85]. There was only one C-terminal mutation ($pilY1_{G1120D}$) located outside of this region. The S59G and G1120D mutations were recapitulated in *P. aeruginosa* PAO1 *ΔpilU* (**Figure 7**). Of these, $pilY1_{G1120D}$ restored twitching motility to 79.6% ± 21.4 of the WT, while the $pilY1_{S59G}$ only restored twitching to 34.2% ± 11.8 (**Figure 7**).

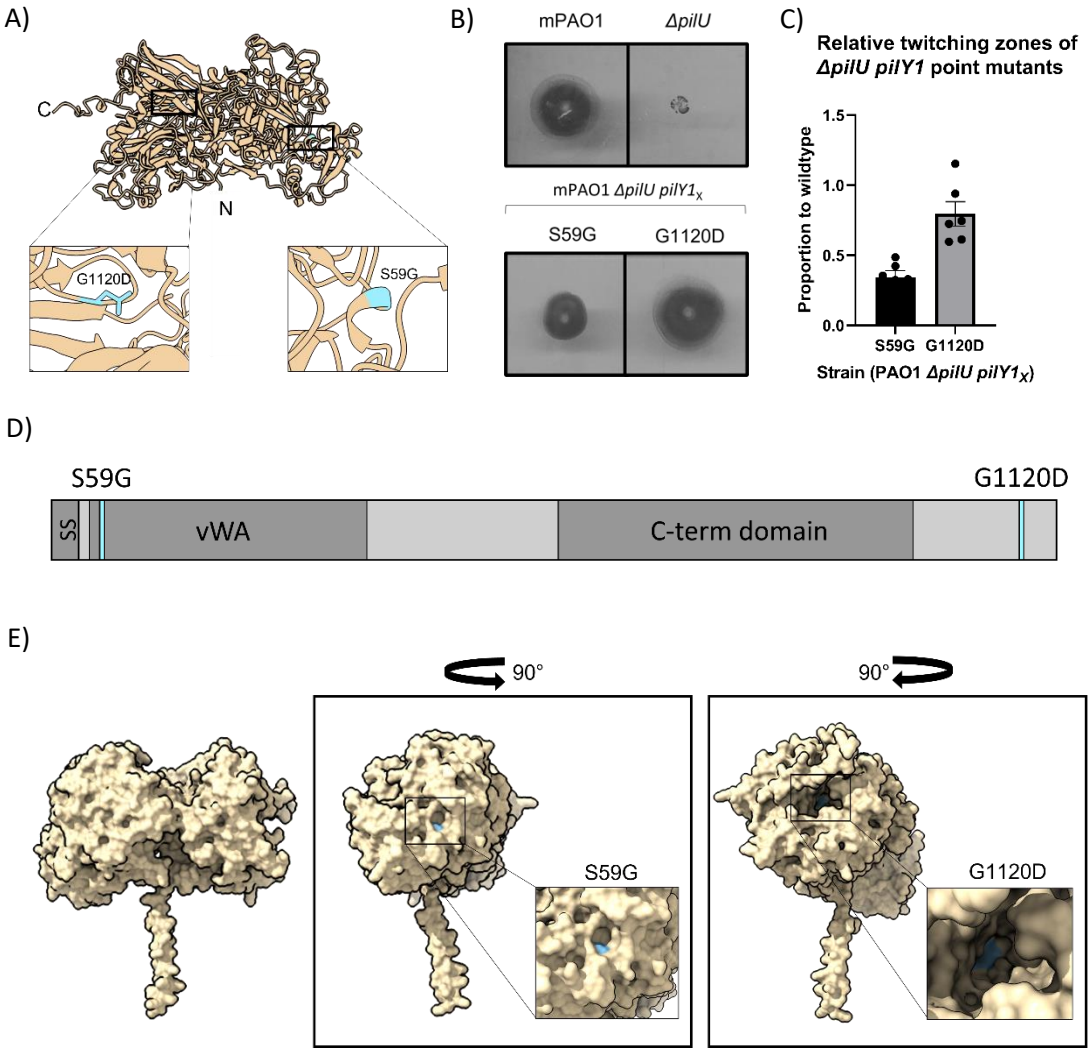

Figure 7. Structural models of PilY1 and representative point mutant twitching zones with quantification. A) An Alphafold2 model of of *P. aeruginosa* PAO1 PilY1 (UniProt: Q9HVM8) represented through ribbons, mutated residues are highlighted in blue [21,22]. B) Representative images from the twitching plates of *ΔpilU pilY1* point mutants after dyeing with crystal violet. C) The twitching zone of *ΔpilU pilY1* point mutants normalized to the wild type *P. aeruginosa* PAO1 per replicate. Bars represent the average of N=2 biological replicates each with 3 technical replicates and error bars are standard error of the mean. D) A linear representation of the PilY1 peptide with mutations highlight in blue. E) An Alphafold2 model of *P. aeruginosa* PAO1 PilY1 (UniProt: Q9HVM8) depicting the surface from forward and 90° clockwise and counter clockwise. Mutated residues are highlighted in blue[21,22]

Strikingly, the gene that was mutated in all but one of the *ΔpilU* gain-of-twitching isolates was *pilA,* encoding the major pilin subunit. Here, mutations in *pilA* are numbered based on the pre-pilin, before processing by PilD. The mutations included $pilA_{M13I}$, $pilA_{P28L}$, $pilA_{V34F}$, $pilA_{A40T}$, $pilA_{G60R}$, $pilA_{N87K}$, and $pilA_{G130E}$. The one exception – $pilC_{V80E}$ – had a mutation in the gene encoding the platform protein, PilC (**Figure 6**). The $pilC_{V80E}$ mutant was the least efficient at twitching (1.8% ± 1.0 of wild-type twitching zone), and was excluded from further analysis. The location of the PilA mutations (not including N87K) on an AlphaFold2 model of the PAO1 pilin is shown in **Figure 8** [21,22]. Of these, only $pilA_{G60R}$ and $pilA_{N87K}$ were identified twice. All mutations except $pilA_{G60R,}$ $pilA_{N87K}$ and $pilA_{G130E}$ are in the α-helical region of PilA. M13I, P28L and V34F are in the α1N region while A40T and P48L are in α1C. The G60R mutation is in the αβ-loop near the α1C region, while N87K is in the αβ-loop but closer to β1. The G130E mutation is between β3 and β4. The only other shared mutation was *bkdB,* which occurred in six of the mutants. The *bkdB* gene encodes a branched-chain alpha-keto acid dehydrogenase[86,87]. BkdB has not been associated with T4P or the regulation of twitching motility[87,88] and this mutation was not further studied.

3.2 Single point mutations in pilA are sufficient to restore twitching in a *ΔpilU* background

Each of the EMS-derived *pilA* mutations that restored motility in the *ΔpilU* mutant was recapitulated in a clean *ΔpilU* background. All single point mutations

restored twitching to between 27-114% compared to wild type (**Figure 9**). Motility of the *ΔpilU pilA*$_{A40T}$ mutant was similar to the parent (114.1% ± 17.5 of wild type). The next best was *pilA*$_{M13I}$, which restored twitching to 51.5% ± 15.6 that of the wildtype.

The *pilA*$_{A40T}$ point mutant twitching was remarkably similar to the wild type. To determine if this was due to the position of the mutation or the properties of the amino acid substituted, we expressed mutant *pilA* with various amino acid substitutions at the A40 position from the arabinose inducible vector pBADGr. These mutations included A40- C, D, G, M, Q, R, S or W. Expression of each pilin was induced using 0.2% arabinose in *ΔpilU* mutants. In preliminary data from one biological and technical replicate, the *pilA*$_{A40-}$, C, D, Q and W substitutions twitched. Replicates of this assay including the original pBADGr-*pilA*$_{A40T}$ control are underway.

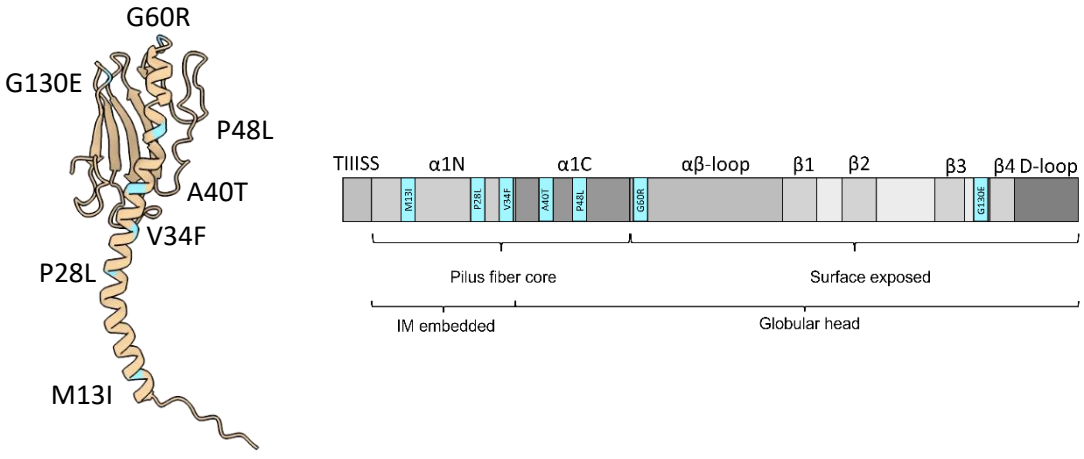

Figure 8. Model and linear diagram of PilA with gain-of-twitching point mutations. A) The *pilA* point mutations mapped onto an AlphaFold 2 model of the *P. aeruginosa* PAO1 prepilin highlighted in blue[21,22]. B) A linear representation of the PilA prepilin peptide, mutated residues are highlighted in blue.

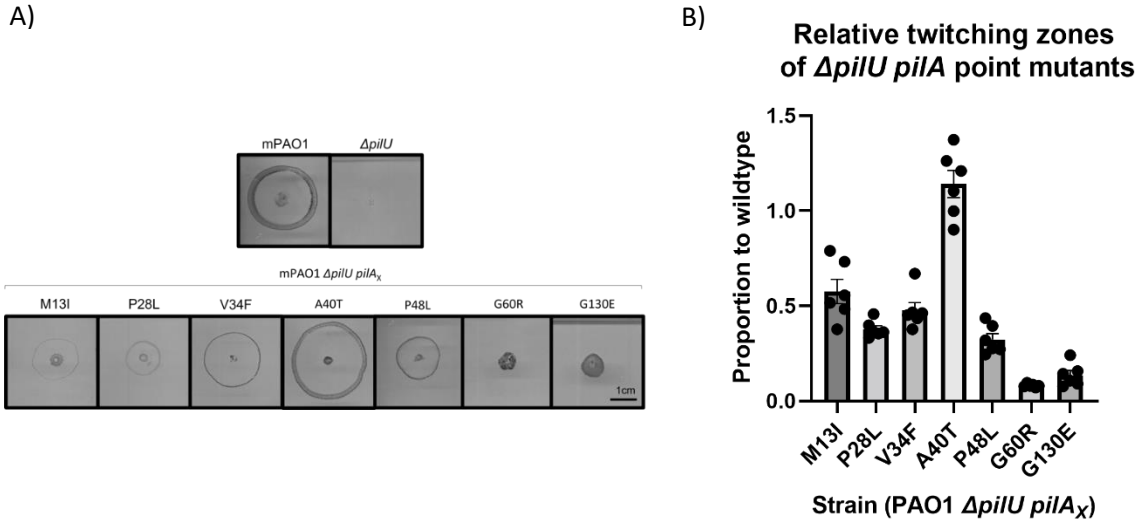

Figure 9. Twitching motility of PAO1 *pilA pilU* mutants. A) Representative images from the twitching plates of *ΔpilU pilA* point mutants after staining with crystal violet. B) The twitching zone of *ΔpilU pilA* point mutants normalized to the wild type *P. aeruginosa* PAO1 per replicate. Bars represent the average of N= 2 biological replicates with 3 technical replicates each and error bars are standard error of the mean.

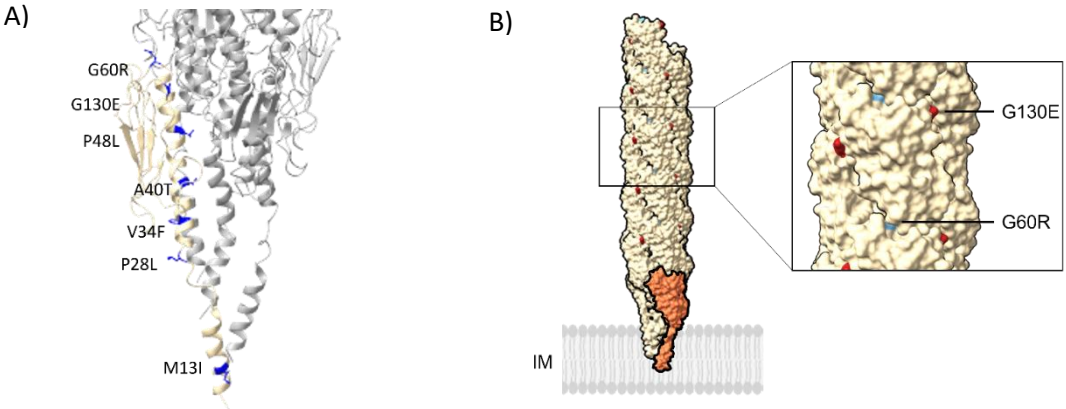

Figure 10. Location of PilA point mutations that restore twitching in the *pilU* background within the pilus fiber. A) The *P. aeruginosa* PAO1 *pilA* mutations mapped onto the structure of a *P. aeruginosa* PAK pilus (PDB: 5VXY)[20]. B) The *P. aeruginosa* PAO1 *pilA* mutations mapped onto a surface representation of a *P. aeruginosa* PAK pilus (PDB: 5VXY)[20]. The mutated residue G60R is coloured blue and G130E is coloured red. A pilin monomer within the fiber is highlighted in orange. Most mutations in PilA are within the helical core of the pilus fiber.

There were two *pilA* point mutations in the αβ ($pilA_{G60R}$) and β3-4 ($pilA_{G130E}$) loops (**Figure 8**). These residues are predicted to be surface exposed, while the remaining mutations are predicted to be embedded within the pilus fiber (**Figure 10**).These loop mutations were the least effective at restoring twitching. The $pilA_{G60R}$ mutant had 8.1% ± 0.9 of wild-type twitching while $pilA_{G130E}$ had 13.6% ± 6.0 of wild-type motility (**Figure 9**). The $pilA_{N87K}$ mutant is still under construction.

To verify that the mutations in *pilA* were solely responsible for restoring twitching, we performed a complementation experiment with wild-type *P. aeruginosa* PAO1 *pilA,* with the hypothesis that motility would be inversely correlated with wild-type pilin expression levels. Expression of *pilA* is tightly regulated by the PilS-PilR two-component system[25]. When there are high levels of PilA in the inner membrane, PilS dephosphorylates PilR, decreasing *pilA* expression[30]. Thus, expression of *pilA in trans* from a plasmid decreases chromosomal expression of *pilA* by increasing total PilA pools in the inner membrane. The arabinose-inducible vector pBADGr was used to titrate the expression of wild-type *pilA.*

As predicted, reintroduction of wild-type PilA decreased twitching in the gain-of-function mutants. Interestingly, the concentration of arabinose at which twitching was inhibited was dependent on the specific *pilA* point mutation (**Figure 11**). In $pilA_{A40T,}$ $pilA_{M13I,}$ and $pilA_{P28L}$, twitching was not abolished even at the highest concentration of arabinose tested. Other mutants lost the ability to twitch at concentrations between

0.05-0.2% arabinose (**Figure 11**).

Recent work on *V. cholerae* competence pili showed that point mutations in the major pilin allowed for both PilT- and PilU-independent retraction, suggesting that the mutant pili were prone to spontaneous disassembly [64]. Therefore, we tested whether a *pilA* point mutation that restored motility in the absence of PilU also allowed for retraction ATPase-independent twitching. Introduction of a *ΔpilT* mutation in the *ΔpilU* $pilA_{A40T}$ background led to loss of motility, suggesting that the motility in the double mutant remains dependent on PilT (**Figure 12**). Twitching motility can be uncoupled from pilus retraction in *pilU*-deficient mutants, as demonstrated through iSCAT microscopy and phage sensitivity assays, implying that the triple mutant might still be capable of a level of pilus retraction that was insufficient for motility[53,62]. Therefore, we tested phage sensitivity of the triple mutant as well. The wild type, *ΔpilU*, and *ΔpilU* $pilA_{A40T}$ strains were phage sensitive, while the *ΔpilT, ΔpilT ΔpilU, ΔpilT ΔpilU* $pilA_{A40T}$, and PAO1 *pilA::*Tn5 strains were resistant (**Figure 13**). These data show that PilT is essential for pilus function in the *ΔpilU* $pilA_{A40T}$ background.

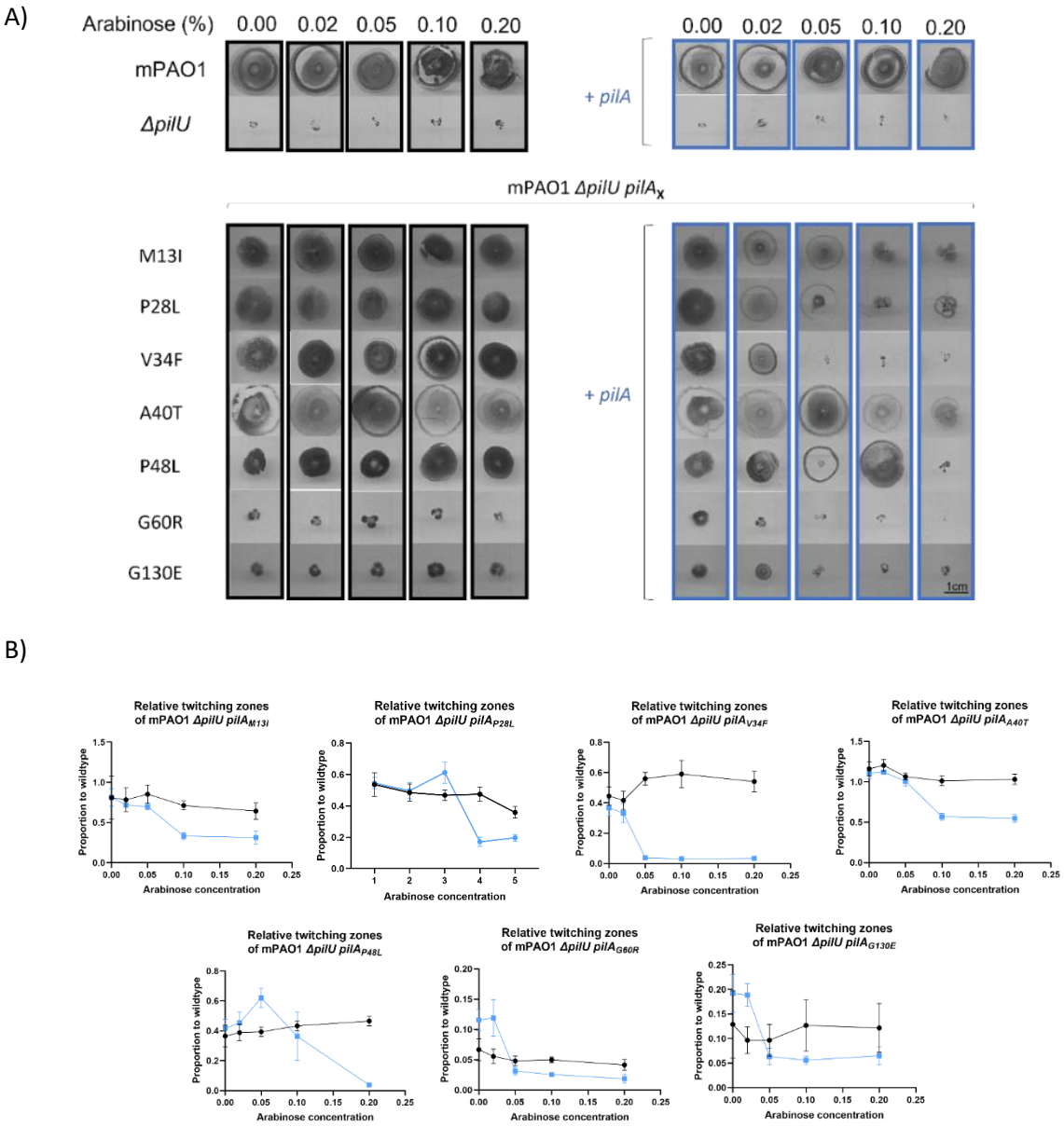

Figure 11. Twitching motility of *ΔpilU pilA* point mutants complemented with wild type *pilA*. A) Representative images of strains containing the pBADGr vector control are outlined in black; strains expressing wild-type *pilA* from pBADGr are outlined in blue. Increasing wild type *pilA* expression leads to loss of twitching in some, but not all, mutant backgrounds. The strains *ΔpilU pilA*$_X$ M13I, P28L and A40T retain twitching at 0.2% arabinose while all *pilA* point mutants lose twitching between 0.05-0.2% arabinose. B) Quantification of the twitching zones of *ΔpilU pilA* point mutants expressing wildtype *pilA* in blue versus the vector control in black. N=3 technical replicates in 2 biological replicates. Error bars are standard error of the mean.

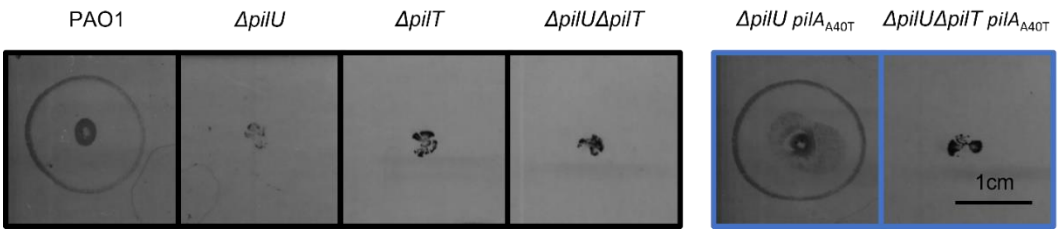

Figure 12. Twitching zones of *P. aeruginosa* PAO1 T4P retraction ATPase deletions. The black borders indicate stains with wildtype PilA, the blue border indicates strains with the *pilA$_{A40T}$* mutation. Deleting *pilT* in a *ΔpilU pilA$_{A40T}$* mutant abolishes twitching motility. N = two biological replicates with 4 technical replicates each.

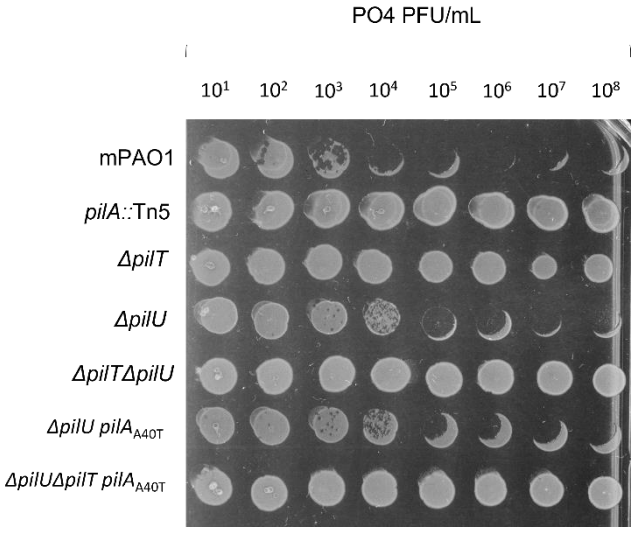

Figure 13. Phage susceptibility of *P. aeruginosa* mPAO1 *ΔpilU* and *ΔpilT* mutants. Six µL of standardized OD_{600} 0.2 *P. aeruginosa* cultures subcultures were first spotted onto 1.5% LB agar then 4 µL of PO4 phage at the indicated PFU/mL was aliquoted directly on top of the bacteria. Plates were incubated at 37°C for 24 h. N=2 technical replicates. Deletion of *pilT* in any background leads to loss of PO4 susceptibility. The *ΔpilU* mutants were ~10 fold less susceptible to PO4 than the wild type.

We next hypothesized that if PilU contributes to pilus retraction, reintroduction of PilU into the gain-of-function *pilA* mutants – especially those that had only partial

restoration of motility – might further increase twitching. To test this idea, *pilU* was expressed *in trans* in the *ΔpilU pilA* point mutant backgrounds. Complementation with PilU had no significant effect on twitching zone expansion except in the $pilA_{M13I}$ background, where PilU increased the twitching zone by ~2x (**Figure 14**). These data suggest that filament disassembly dynamics rely on a combination of PilU function and PilA subunit-subunit interactions.

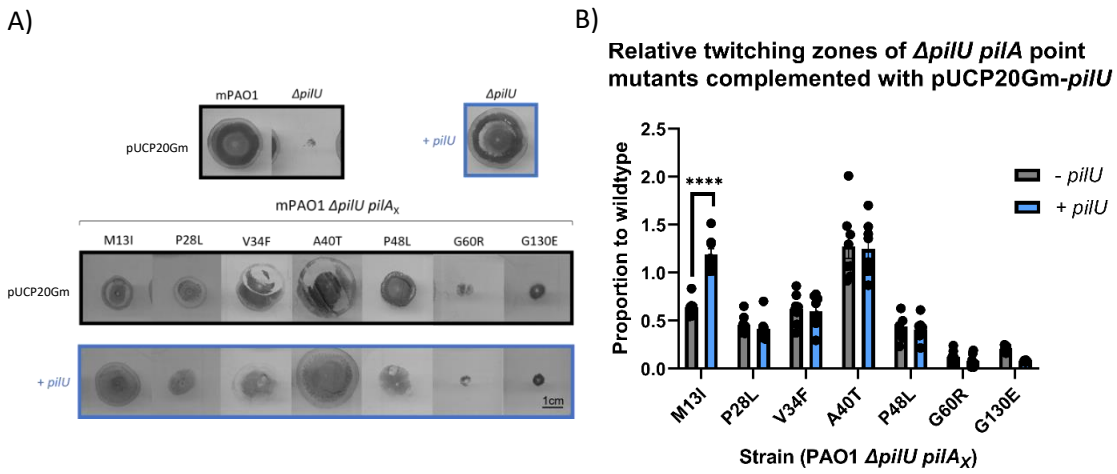

Figure 14. Complementation of *ΔpilU pilA* point mutants with pUCP20Gm-*pilU* A) Representative images from the twitching plates of *ΔpilU pilA* point mutants after staining with crystal violet. Strains complemented with PilU are outlined in blue, strains with the empty pUCP20Gm vector are outlined in black. B) The relative twitching zones of *pilA* point mutant strains complemented with PilU. Complementation with PilU did not significantly impact the twitching zones of mutants relative to the wild-type control except for in the $pilA_{M13I}$ mutant ($p < 0.0001$). Complementation increased the relative twitching zone of $pilA_{M13I}$ from 64.1% ± 9.0 to 119.2% ± 17.3. N = 2 biological replicates, each with 4 technical replicates.

3.3 Colony morphology of PilA point mutants resembles that of the *ΔpilU* parent strain

T4P have multiple functions, including contributing to surface sensing[62]. When

pili contact a surface, a signal cascade is triggered via a poorly understood pathway that ultimately results in the upregulation of the second messengers cAMP and c-di-GMP to promote the expression of EPS and other factors contributing to biofilm formation and virulence[62]. *ΔpilU* mutant colonies have a small rugose phenotype, while wild-type *P. aeruginosa* PAO1 grows as large smooth colonies. These differences in colony phenotypes have been attributed to differences in exopolysaccharide production[63]. Pilus depolymerization in *P. aeruginosa* is hypothesized to be most efficient with two retraction ATPases (PilT and PilU), and the loss of PilU may skew retraction dynamics, phenocopying the trapping of pili outside the cell upon surface contact. In turn, loss of PilU might result in the upregulation of second messengers and exopolysaccharide synthesis, offering an explanation for the phenotypic differences between wild type and *ΔpilU* colonies. Restoration of motility in a background lacking PilU allowed us to ask whether pilus retraction alone was sufficient to restore normal surface sensing and wild-type colony morphology, or if PilU plays a more direct role.

Despite the restoration of twitching, several double mutants retained the characteristic *ΔpilU* colony morphology (**Figure 15a**). When complemented with *pilU in trans,* the twitching *ΔpilU pilA* point mutants exhibited a intermediate colony morphology compared to the wild type or *ΔpilU* parent strain. The *pilU*-complemented strains formed large colonies like wild-type *P. aeruginosa,* but they were matte instead of glossy. This was also true for the complemented *ΔpilU* parent strain, suggesting that despite restoring motility, expression of PilU *in trans* does not recapitulate wild-type

surface signalling, a potential consequence of overexpression (**Figure 15b**). From preliminary work with the PilY1 mutations S59G and G1120D in a *ΔpilU* background (data not shown) these double mutants have a colony morphology resembling *in trans pilU* expression.

A)

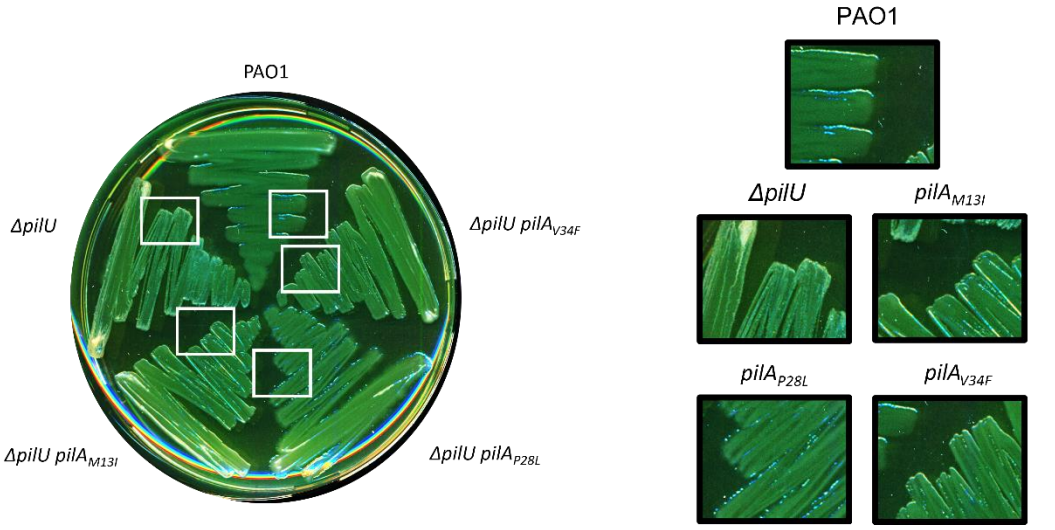

B)

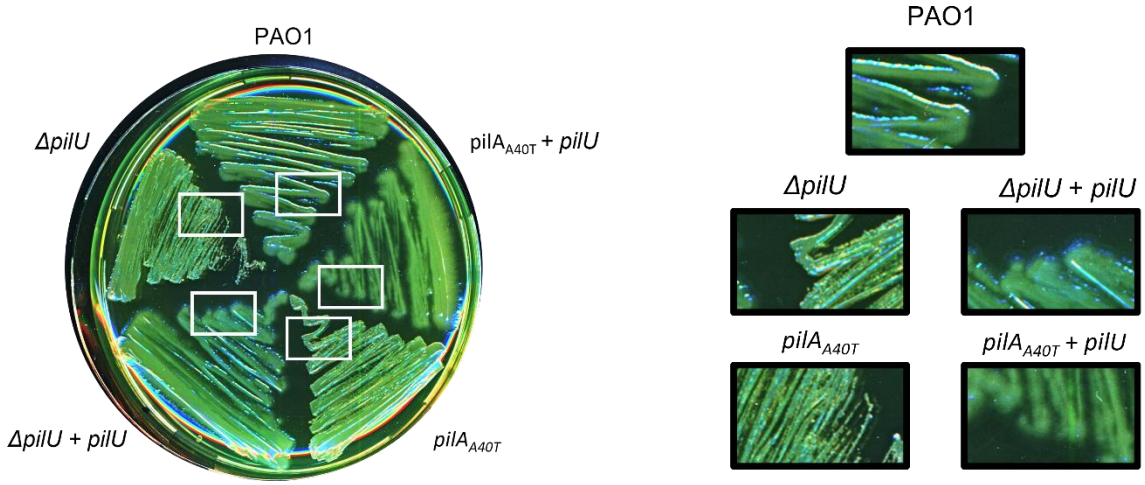

Figure 15. Samples of representative images of *P. aeruginosa ΔpilU pilA* point mutant colony morphology. A) Phenotypes of WT *P. aeruginosa* PAO1, *pilU*, and *pilU pilA* point mutant (M13I, P28L, V34F) cultures. B) Phenotypes *pilU* and *pilU* $pilA_{A40T}$ point mutant cultures complemented with *pilU* compared to WT *P. aeruginosa* PAO1 with an empty vector. Cells were streaked on LB agar and incubated at 37°C for 12 h prior to imaging with a flatbed scanner. Representative Images of all *pilA* point mutant cultures are in **Supplementary Figure 3.**

Congo red is a diazo dye that binds EPS, conferring a pink/red colour on colonies that overproduce polysaccharides and making it easier to visualize rugose colony phenotypes, Coomassie blue was added to increase the contrast between colonies and the media[80]. A Congo red assay using the gain-of-twitching mutants revealed a range of Congo red binding and diverse colony morphologies which did not correlate with the degree to which twitching was restored (**Figure 16**). These data suggest that both PilA and PilU contribute to surface sensing, and that changes to PilA sequence can impact signalling independently from twitching motility.

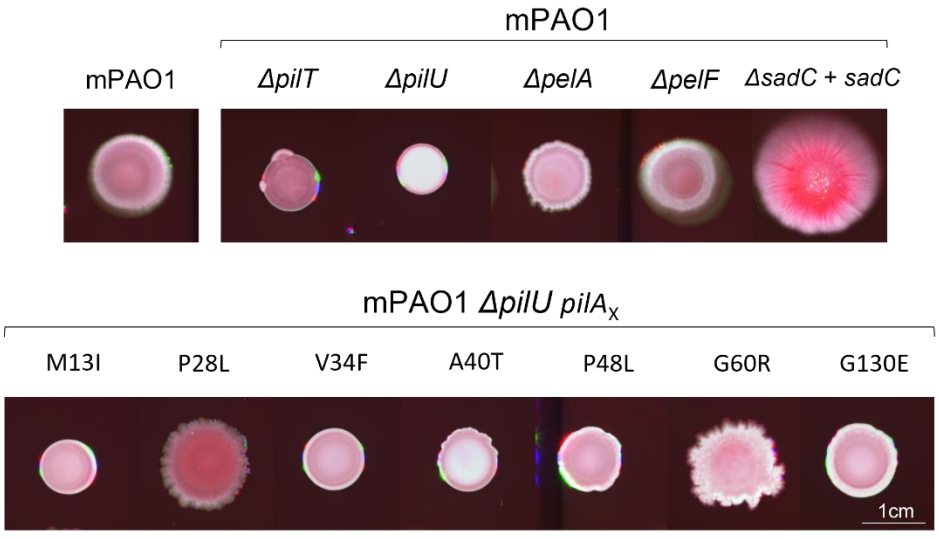

Figure 16. Representative Congo red binding assays. Cultures were grown to OD_{600} 0.6 and diluted to 1/100 in 1 x PBS then 5 µL were aliquoted onto TSB containing 40 µg/mL

Congo red and 15 μg/mL Coomassie blue 1.5% agar. Plates were incubated at 25°C for 5 days before imaging.

3.4 No pulling event for *ΔpilU* mutants in preliminary analysis of polyacrylamide micropillar assays

To directly measure the contribution of PilU to force generation during pilus retraction, we collaborated with the Biais lab to perform polyacrylamide micropillar (PoMP) assays. The assay requires that all strains lack flagella, to prevent false positives from the flagella displacing the micropillars [89]. We created *ΔfliC* (flagellin) mutants of each of the strains of interest and verified lack of flagellum expression using a surface-shearing assay and SDS-PAGE gel (**Supplementary Figure 2a**). Strains used for the micropillar assay were verified to be piliated using the same method, confirmed by Western blot using anti-PilA sera (Supplementary figure 2b). In preliminary observations from the PoMP assay, there was no displacement of micropillars by the *ΔpilU* or *ΔpilT* mutants, but frequent displacement of micropillars by WT *P. aeruginosa* mPAO1. All PoMP micropillar assays for the strains mentioned have been completed, and the results are currently being analyzed.

CHAPTER 4. DISCUSSION

4.1 PilU is dispensable for twitching motility

Here we show that PilU is dispensable for twitching motility in *P. aeruginosa*, and that multiple gain-of-function mutations can be mapped to two components of the pilus filament, the major pilin PilA and the pilus adhesin PilY1. A recent study describing

motor-independent retraction of *V. cholerae* competence pili identified point mutations in the major pilin gene (*pilA*) that restored retraction in a retraction ATPase (PilT)-deficient background [64]. Restoration of retraction was attributed to lower affinity interactions among subunits in the pilus filament resulting from the substitution of bulkier amino acids such as Ser in place of Gly[64]. *V. cholerae* does not require PilU for twitching motility and cannot be compared directly to *P. aeruginosa*, but the notion that retraction can be governed by inherent properties of the pilus fiber is supported by our discovery that *pilA* point mutations can restore motility in a *pilU* background[64]. Determining how *pilA* mutations compensate for the loss of PilU can then be used to shed light on its function. It is possible that the mutations identified here reduce subunit-subunit affinity as proposed by Chlebek et al. (2021), making the filament easier to depolymerize[64]. We also found substitutions of small amino acids such as Gly and Pro with Arg, Glu, and Leu (*pilA*$_{G60R}$, *pilA*$_{G130E}$, *pilA*$_{P28L}$, *pilA*$_{P48L}$). These data are consistent with the idea that PilU may contribute to the force necessary for depolymerization of the pilus fiber under tension, as pili retraction in *ΔpilU* mutants has been observed directly in liquid media through iSCAT microscopy [53,62].

Most of the *pilA* point mutations that restore twitching motility in the *pilU* background are in the N-terminal α-helix of PilA (**Figure 8**). Hydrophobic interactions between the α-helices of adjacent pilins are thought to contribute to its ability to withstand the forces generated during retraction following surface adhesion[11,13]. The mutations in this region restore twitching to a greater extent than those in the C-

terminal domain. Many of the substitutions in the A40 position also restored twitching. All the amino acid substitution in the A40 position that restore twitching are larger than alanine (Cys, Asp, Gln, and Trp) but had no clear pattern with regards to charge and polarity, and other amino acids with similar structures and charges (Gly, Met, Arg, Ser) do not restore twitching. These data are preliminary, but suggest that the potential disruption of interactions with pilin helices is contingent on the nature and position of the substitutions.

The C-terminus of PilA is exposed to the extracellular environment, and its composition impacts the surface chemistry and related functions of the pilus[11,13]. The C-termini of pilins are highly variable. Mutations in this region are least effective in restoring twitching, potentially because the interactions between the loops of adjacent subunits are less critical in controlling inter-subunit packing and therefore have less influence over pili dynamics. In *Neisseria meningitidis,* specific mutations in the conserved N-terminal of the major pilin protein (PilE) result in short pili that prevent cell-cell aggregation but did not interfere with surface adhesion[90]. Conversely, mutations in the C-terminus of PilE interfere with adhesion to surfaces but do not influence the length of pili[90]. It is possible that shorter *N. meningitidis* pili are a consequence of disruptions in pilin interactions that result in unstable, easily collapsible pili. This would agree with the model proposed by Chlebek et al. (2021), and the data described here [64,91].

In contrast to the motor-independent retraction described by Chlebek et al. (2021) the loss of twitching motility and phage sensitivity in the PAO1 *ΔpilT ΔpilU pilA*$_{A40T}$ mutant support a model where PilT is still required for pilus disassembly in *P. aeruginosa*. These data suggest PilU may be modulating the force of retraction, but at a level undetectable by PoMP assays. This work is still preliminary, and no concrete conclusions can yet be drawn; however, it is a promising direction in determining the function of PilU.

The discovery of PilY1 mutations that restore twitching motility in the absence of PilU is novel. The low copy number and large size of PilY1 (~125 kDa) makes the gain-of-twitching phenotype of single amino acid mutations very striking. The gain-of-function of PilY1 S59G and G1120D was recapitulated in a clean *ΔpilU* background. S59G is in the vWA domain, and G1120D is outside domains of known function. PilY1 in *P. aeruginosa* contains 5 conserved Cys residues, the majority of which lie within the vWA domain. These Cys residues are proposed to form disulphide bonds that, like those in the von Willebrand factor in eukaryotes, can break under mechanical stress, causing a conformational change that allows PilY1 to relay a signal for surface contact[19,84]. Mutating the Cys residues in the vWA domain of PilY1 reduces the length of time that pili remain adhered to a surface, but does not impair twitching motility[84]. PilY1 S59G may interfere with a conformational change and prevent pili from adhering to surfaces for extended periods of time. Likewise, the G1120D mutation is adjacent to the C-terminal region (residues 585-997) that is proposed to be the adhesive component of

PilY1[83–85]. The G1120D mutation restored twitching motility to a greater extent than S59G. G1120D might interfere with PilY1 adhesion to surfaces as well. We hypothesize that mutations in PilY1 might interfere with its adhesion to surfaces, resulting in more frequent detachment and retraction and allowing bacteria to twitch across surfaces with "shorter steps".

4.2 Twitching motility and surface sensing can be genetically separated

Pilus retraction is commonly associated with surface sensing, but the mechanism of signal transduction is poorly understood[92,93]. Upregulation of cAMP production is associated with activation of the Pil-Chp system, but the ligand/signal recognized by the MCP PilJ is unknown[17]. The signal for regulation of the second messenger c-di-GMP is also unknown but is proposed to be transmitted via PilY1 through the alignment subcomplex PilMNOP to increase SadC expression for c-di-GMP production[17]. All these mechanisms rely on pilus retraction, which requires ATPase motors PilT and PilU in *P. aeruginosa*. *P. aeruginosa pilU* mutants constitutively upregulate cAMP production while *pilT* mutants do not[17,61]. Further, *pilU* mutants have upregulated exopolysaccharide expression, which is positively correlated with c-di-GMP levels and results in a unique rugose colony phenotype[61,63]. As observed through iSCAT microscopy *pilU* mutants retract pili at the same rate as wild type in liquid, but are unable to twitch across surfaces[62]. One interpretation of these data is that PilU contributes to surface sensing. Here we describe *ΔpilU* "gain-of-twitching" mutants that still have dysregulated

exopolysaccharide production despite the restoration of pili function (**Figure 16**), suggesting that motility and sensing by pili are independent functions.

CHAPTER 5. CONCLUSIONS AND FUTURE DIRECTIONS

5.1 Conclusions

Here we described several mutations in type IV pilus fiber proteins that can restore twitching in *ΔpilU* mutants. Many of these mutations were in the major pilin protein PilA, which is the most abundant in the pilus fiber. These mutations restored twitching to varying degrees, seemingly dependent on their location on the pilin, with those in the N-terminal domain restoring twitching to the greatest extent. The PilA A40 substitutions results suggest that both the location and nature of an amino acid substitution contributes significantly to twitching restoration. No micropillar displacement was observed in the preliminary analysis of the PoMP for *ΔpilT* and *ΔpilU* mutants, and the gain-of-twitching $pilA_{A40T}$ point mutant phage susceptibility was PilT-dependent. Together these results suggest PilU might be modulating the force of retraction at a level undetectable by the PoMP assay. This aligns with the hypothesis that point mutations in PilA disrupt interactions between adjacent monomers, making the fiber easier to depolymerize. Strikingly, twitching motility could be uncoupled from exopolysaccharide production, suggesting PilU might have a distinct role in surface sensing. Mutations in the adhesin protein PilY1 also restored twitching motility, which

might be a consequence of altered adhesiveness. The discovery of these mutations is very interesting given the low copy number and large size of PilY1 and this finding is novel to the field of T4P. Much more work is needed to determine how these mutations contribute to T4P dynamics; possible experiments are outlined in the following sections.

5.2 Determine if all gain-of-twitching point mutations are PilT dependent

As described in this thesis, the gain-of-twitching mutation $pilA_{A40T}$ is dependent on the retraction ATPase PilT. Deleting *pilT* resulted in a loss of twitching and phage sensitivity, indicating that pili were no longer being retracted. Because motor independent retraction has been described in *V. cholerae* these results cannot be generalized without further investigation of PilT-dependence in the remaining gain-of-function mutants[64]. The construct for deleting *pilT* in *ΔpilU* mutants has already been made and verified. It would be prudent to determine if all these gain-of-twitching mutations require PilT via twitching and phage susceptibility assays. If no *ΔpilT* mutants are phage susceptible, we can conclude that this set of gain-of-twitching point mutations is dependent on PilT. It would be interesting to repeat the EMS mutagenesis experiment in a *ΔpilTΔpilU* mutant to ascertain if motor independent twitching motility is possible in *P. aeruginosa*.

5.3 PoMP assay with pilA point mutations and pilU complementation

We hypothesized that that the *pilA* point mutations allow for easier disassembly of pili, and preliminary data from the PoMP indicates that PilU contributes to the force

of retraction. The “gain of twitching” mutants may exhibit retractive forces in this assay that correlate with how well they twitch compared to the wild type. *fliC* knockout strains in *ΔpilU pilA*$_{G60R}$ and *ΔpilU pilA*$_{P48L}$ backgrounds were constructed and sent to the Biais lab; results are pending. Other mutants of interest include *pilA*$_{A40T}$ and *pilA*$_{M13I}$; together these strains provide a range of twitching in the *pilU* background. To further demonstrate that PilU is important for force generation, the micropillar experiments can be repeated using *ΔpilU* and *ΔpilU pilA* point mutation backgrounds expressing *pilU in trans*. Our existing pUCP20Gm-*pilU* plasmid fully complements twitching in *pilU* mutants and could be introduced into these backgrounds to measure the force of retraction.

Dynamics studies of fluorescently labelled pili from *V. cholerae* showed that some of the motor-independent retraction pilin mutations resulted in shorter pili[64]. Pilus length is a limiting factor for the PoMP assay, as a pilus must be long enough to contact a neighbouring micropillar; thus, retraction events from short pilus fibers are not detectable[89]. There are other techniques to measure the force of pilus retraction such as an optical tweezer assay. Briefly, that assay uses a microscope to trap a carboxylated silica or latex bead (dielectric materials) at a fixed location with intense light that generates a three-dimensional gradient of electromagnetic energy [89]. No force is exerted on the bead while it is in the center of the optical trap, when pili adhere to a bead and are retracted, a restoring force is exerted on the bead by the optical trap [89]. The distance that the bead can be displaced by pilus retraction is directly related to the force

generated [89]. This is a potential option if the pili in our mutants are too short for the PoMP assay.

5.4 Cysteine substitution labeling of gain-of-twitching mutant pili

Pilus dynamics in live cells can observed by the substitution of a surface-exposed residue on the major pilin with a Cys which can then be labeled with thiol-reactive fluorescent maleimide dyes[94]. The substitution of Ser or Thr in the globular head region of PilA with Cys has facilitated imaging of *in vivo* pilus dynamics for *P. aeruginosa*, *V. cholerae*, *Caulobacter crescentus,* and other bacteria[94]. In *P. aeruginosa* PAO1, the substitution of Thr107 (numbered based on the pre-pilin) with Cys allows labeling with maleimide dye without significantly impeding twitching motility (Burrows, unpublished). Knock-in constructs for $pilA_{T107C}$, $pilA_{A40T\ T107C}$, $pilA_{V34F\ T107C}$ and $pilA_{P48L\ T107C}$ have been generated and verified to have the correct sequence. Knock-in mutants with both gain-of-twitching and Cys substitution mutations can be used to determine the length of pili (important for interpretation of the PoMP assay results) and the frequency of pili retraction. For the *pilY1* mutants, determining the frequency of retraction using labeled pilins will aid in testing the hypothesis that mutants are twitching via more frequent but short-lived extension-retraction events.

In addition to visualizing pili in real time, the same Cys substitutions can be labeled with large maleimide-conjugated molecules such as PEG, which disrupts pili dynamics by obstructing retraction of extended pili[94,95]. By obstructing the retraction of

pili in *ΔpilU* gain-of-twitching mutants and measuring the levels of second messengers cAMP and c-di-GMP, it will be possible to determine if the dysregulation of these messengers is a consequence of the *pilU* deletion or alterations in pilus dynamics. This would help to explain the observations from the Congo red assay, which suggest that motility and surface signalling are not correlated (**Figure 16**).

5.5 Measuring pilin monomer interactions within the fiber with pilA point mutations

The Dalia lab hypothesized that changes in the interaction between pilin monomers resulted in a less stable fiber that could spontaneously collapse, but did not formally test this hypothesis [64]. Here we described similar gain-of-function for twitching motility facilitated by mutations in *pilA*, implying a similar mechanism. The strength of interaction between pilin monomers in a fiber can be estimated by thermal stability and chemical stability [96]. In a previous study comparing the stability of T4aP versus T4bP, the thermal stability of pilus fibers was measured using circular dichroism (CD) spectroscopy over a temperature gradient of 22-80°C. Denaturation of pilus fibers was marked by a sudden increase in molar ellipticity[96]. Similarly, the chemical stability of T4aP versus T4bP was compared using increasing concentrations of urea. These techniques can be applied to the gain-of-twitching pili described in this work to determine if these mutations disrupt the pilus structure.

5.6 Measuring adhesive properties of mutant pili

Atomic force microscopy (AFM) can be used as a quantitative probe to measure the force of interaction and physical properties of biomolecules[97]. To measure the adhesive strength of pili, bacterial cells can be fixed to a surface and a cantilever probe with an adhesive coating such as poly-L-lysine can be lowered onto a pili, pulling it from the surface and measuring the force required to displace it over time[84,97]. AFM has been used to measure the adhesiveness of PilY1 effectively in the past, being able to define two types of adhesive behaviour; spikes and steps, which are attributed to nano-spring behaviour and lengthening of the pili (including PilY1) respectively[84]. This method can be employed again to investigate the adhesive properties of mutant PilY1 and PilA, adding to our understanding of why twitching can be restored.

CHAPTER 6. REFERENCES

1. Giltner, C. L., Nguyen, Y. & Burrows, L. L. Type IV Pilin Proteins: Versatile Molecular Modules. *Microbiol. Mol. Biol. Rev.* (2012) doi:10.1128/mmbr.00035-12.
2. Imam, S., Chen, Z., Roos, D. S. & Pohlschröder, M. Identification of surprisingly diverse type IV Pili, across a broad range of gram-positive bacteria. *PLoS One* (2011) doi:10.1371/journal.pone.0028919.
3. Burrows, L. L. Weapons of mass retraction. *Molecular Microbiology* (2005) doi:10.1111/j.1365-2958.2005.04703.x.
4. Hahn, H. P. The type-4 pilus is the major virulence-associated adhesin of *Pseudomonas aeruginosa* - A review. in *Gene* (1997). doi:10.1016/S0378-1119(97)00116-9.
5. Scheurwater, E. M. & Burrows, L. L. Maintaining network security: How macromolecular structures cross the peptidoglycan layer. *FEMS Microbiology*

Letters (2011) doi:10.1111/j.1574-6968.2011.02228.x.

6. Boyd, J. M. Localization of the histidine kinase PilS to the poles of *Pseudomonas aeruginosa* and identification of a localization domain. *Mol. Microbiol.* (2000) doi:10.1046/j.1365-2958.2000.01836.x.

7. Treuner-Lange, A. *et al.* PilY1 and minor pilins form a complex priming the type IVa pilus in *Myxococcus xanthus. Nat. Commun.* (2020) doi:10.1038/s41467-020-18803-z.

8. Nguyen, Y. *et al. Pseudomonas aeruginosa* minor pilins prime type IVa pilus assembly and promote surface display of the PilY1 adhesin. *J. Biol. Chem.* (2015) doi:10.1074/jbc.M114.616904.

9. Giltner, C. L., Habash, M. & Burrows, L. L. *Pseudomonas aeruginosa* minor pilins are incorporated into type IV Pili. *J. Mol. Biol.* (2010) doi:10.1016/j.jmb.2010.03.028.

10. Maier, B., Potter, L., So, M., Seifert, H. S. & Sheetz, M. P. Single pilus motor forces exceed 100 pN. *Proc. Natl. Acad. Sci. U. S. A.* (2002) doi:10.1073/pnas.242523299.

11. Craig, L., Pique, M. E. & Tainer, J. A. Type IV pilus structure and bacterial pathogenicity. *Nature Reviews Microbiology* (2004) doi:10.1038/nrmicro885.

12. Biais, N., Ladoux, B., Higashi, D., So, M. & Sheetz, M. Cooperative retraction of bundled type IV pili enables nanonewton force generation. *PLoS Biol.* (2008) doi:10.1371/journal.pbio.0060087.

13. Craig, L. & Li, J. Type IV pili: paradoxes in form and function. *Current Opinion in Structural Biology* (2008) doi:10.1016/j.sbi.2007.12.009.

14. Marko, V. A., Kilmury, S. L. N., MacNeil, L. T. & Burrows, L. L. *Pseudomonas aeruginosa* type IV minor pilins and PilY1 regulate virulence by modulating FimS-AlgR activity. *PLoS Pathog.* (2018) doi:10.1371/journal.ppat.1007074.

15. Strom, M. S., Bergman, P. & Lory, S. Identification of active-site cysteines in the conserved domain of PilD, the bifunctional type IV pilin leader peptidase/N-methyltransferase of *Pseudomonas aeruginosa*. *J. Biol. Chem.* (1993).

16. Belete, B., Lu, H. & Wozniak, D. J. *Pseudomonas aeruginosa* AlgR regulates type IV pilus biosynthesis by activating transcription of the fimU-pilVWXY1Y2E operon. *J. Bacteriol.* (2008) doi:10.1128/JB.01623-07.

17. Luo, Y. *et al.* A hierarchical cascade of second messengers regulates *Pseudomonas aeruginosa* Surface Behaviors. *MBio* (2015) doi:10.1128/mBio.02456-14.

18. Burrows, L. L. *Pseudomonas aeruginosa* twitching motility: Type IV pili in action.

Annual Review of Microbiology (2012) doi:10.1146/annurev-micro-092611-150055.

19. Webster, S., Wong, L., O'Toole, G., & Mohamed, Y. E.-N. The Power of Touch: Type 4 Pili, the von Willebrand A Domain, and Surface Sensing by *Pseudomonas aeruginosa*. *J. Bacteriol.* **204**, e00084-22 (2022).

20. Wang, F. *et al.* Cryoelectron Microscopy Reconstructions of the *Pseudomonas aeruginosa* and *Neisseria gonorrhoeae* Type IV Pili at Sub-nanometer Resolution. *Structure* **25**, 1423-1435.e4 (2017).

21. Jumper, J. *et al.* Highly accurate protein structure prediction with AlphaFold. *Nature* **596**, 583–589 (2021).

22. Varadi, M. *et al.* AlphaFold Protein Structure Database: massively expanding the structural coverage of protein-sequence space with high-accuracy models. *Nucleic Acids Res.* **50**, D439–D444 (2022).

23. Jacobsen, T., Bardiaux, B., Francetic, O., Izadi-Pruneyre, N. & Nilges, M. Structure and function of minor pilins of type IV pili. *Med. Microbiol. Immunol.* **209**, 301–308 (2020).

24. Van Schaik, E. J. *et al.* DNA binding: A novel function of *Pseudomonas aeruginosa* type IV pili. *J. Bacteriol.* (2005) doi:10.1128/JB.187.4.1455-1464.2005.

25. Kilmury, S. L. N., Burrows, L. L., & Harwood., C. The *Pseudomonas aeruginosa* PilSR Two-Component System Regulates Both Twitching and Swimming Motilities. *MBio* **9**, e01310-18 (2018).

26. Boyd, J. M., Koga, T. & Lory, S. Identification and characterization of PilS, an essential regulator of pilin expression in *Pseudomonas aeruginosa*. *MGG Mol. Gen. Genet.* (1994) doi:10.1007/BF00284205.

27. Whitchurch, C. B., Alm, R. A. & Mattick, J. S. The alginate regulator AlgR and an associated sensor FimS are required for twitching motility in *Pseudomonas aeruginosa*. *Proc. Natl. Acad. Sci. U. S. A.* (1996) doi:10.1073/pnas.93.18.9839.

28. Ethier, J. & Boyd, J. M. Topological analysis and role of the transmembrane domain in polar targeting of PilS, a *Pseudomonas aeruginosa* sensor kinase. *Mol. Microbiol.* **38**, 891–903 (2000).

29. Klose, K. E., Weiss, D. S. & Kustu, S. Glutamate at the site of phosphorylation of nitrogen-regulatory protein NTRC mimics aspartyl-phosphate and activates the protein. *J. Mol. Biol.* **232**, 67–78 (1993).

30. Kilmury, S. L. N. & Burrows, L. L. Type IV pilins regulate their own expression via direct intramembrane interactions with the sensor kinase PilS. *Proc. Natl. Acad.*

Sci. U. S. A. (2016) doi:10.1073/pnas.1512947113.

31. Boyd, J. M. & Lory, S. Dual function of PilS during transcriptional activation of the *Pseudomonas aeruginosa* pilin subunit gene. *J. Bacteriol.* (1996) doi:10.1128/jb.178.3.831-839.1996.

32. Ishimoto, K. S. & Lory, S. Identification of pilR, which encodes a transcriptional activator of the *Pseudomonas aeruginosa* pilin gene. *J. Bacteriol.* (1992) doi:10.1128/jb.174.11.3514-3521.1992.

33. Jin, S., Ishimoto, K. S. & Lory, S. PilR, a transcriptional regulator of piliation in *Pseudomonas aeruginosa*, binds to a cis-acting sequence upstream of the pilin gene promoter. *Mol. Microbiol.* (1994) doi:10.1111/j.1365-2958.1994.tb01338.x.

34. West, S. E. H., Sample, A. K. & Runyen-Janecky, L. J. The vfr gene product, required for *Pseudomonas aeruginosa* exotoxin A and protease production, belongs to the cyclic AMP receptor protein family. *J. Bacteriol.* (1994) doi:10.1128/jb.176.24.7532-7542.1994.

35. J., K. M. *et al.* Mechanotaxis directs *Pseudomonas aeruginosa* twitching motility. *Proc. Natl. Acad. Sci.* **118**, e2101759118 (2021).

36. Darzins, A. Characterization of a *Pseudomonas aeruginosa* gene cluster involved in pilus biosynthesis and twitching motility: sequence similarity to the chemotaxis proteins of enterics and the gliding bacterium *Myxococcus xanthus*. *Mol. Microbiol.* (1994) doi:10.1111/j.1365-2958.1994.tb00296.x.

37. Hazelbauer, G. L., Falke, J. J. & Parkinson, J. S. Bacterial chemoreceptors: high-performance signaling in networked arrays. *Trends in Biochemical Sciences* (2008) doi:10.1016/j.tibs.2007.09.014.

38. Whitchurch, C. B. *et al.* Characterization of a complex chemosensory signal transduction system which controls twitching motility in *Pseudomonas aeruginosa*. *Mol. Microbiol.* (2004) doi:10.1111/j.1365-2958.2004.04026.x.

39. Silversmith, R. E., Wang, B., Fulcher, N. B., Wolfgang, M. C. & Bourret, R. B. Phosphoryl Group Flow within the *Pseudomonas aeruginosa* Pil-Chp Chemosensory System: DIFFERENTIAL FUNCTION OF THE EIGHT PHOSPHOTRANSFERASE AND THREE RECEIVER DOMAINS *. *J. Biol. Chem.* **291**, 17677–17691 (2016).

40. Takhar, H. K., Kemp, K., Kim, M., Howell, P. L. & Burrows, L. L. The platform protein is essential for type IV pilus biogenesis. *J. Biol. Chem.* (2013) doi:10.1074/jbc.M113.453506.

41. Karuppiah, V., Hassan, D., Saleem, M. & Derrick, J. P. Structure and

oligomerization of the PilC type IV pilus biogenesis protein from *Thermus thermophilus*. *Proteins Struct. Funct. Bioinforma.* (2010) doi:10.1002/prot.22720.

42. McCallum, M., Tammam, S., Khan, A., Burrows, L. L. & Lynne Howell, P. The molecular mechanism of the type IVa pilus motors. *Nat. Commun.* (2017) doi:10.1038/ncomms15091.

43. Chang, Y. W. *et al.* Architecture of the type IVa pilus machine. *Science (80-.).* (2016) doi:10.1126/science.aad2001.

44. Koch, M. D., Fei, C., Wingreen, N. S., Shaevitz, J. W. & Gitai, Z. Competitive binding of independent extension and retraction motors explains the quantitative dynamics of type IV pili. *Proc. Natl. Acad. Sci.* **118**, e2014926118 (2021).

45. Iyer, L. M., Makarova, K. S., Koonin, E. V. & Aravind, L. Comparative genomics of the FtsK-HerA superfamily of pumping ATPases: Implications for the origins of chromosome segregation, cell division and viral capsid packaging. *Nucleic Acids Research* (2004) doi:10.1093/nar/gkh828.

46. Chiang, P. *et al.* Functional role of conserved residues in the characteristics secretion NTPase motifs of the *Pseudomonas aeruginosa* type IV pilus motor proteins PilB, PilT and PilU. *Microbiology* (2008) doi:10.1099/mic.0.2007/011320-0.

47. Walker, J. E., Saraste, M., Runswick, M. J. & Gay, N. J. Distantly related sequences in the alpha- and beta-subunits of ATP synthase, myosin, kinases and other ATP-requiring enzymes and a common nucleotide binding fold. *EMBO J.* (1982) doi:10.1002/j.1460-2075.1982.tb01276.x.

48. Robien, M. A., Krumm, B. E., Sandkvist, M. & Hol, W. G. J. Crystal structure of the extracellular protein secretion NTPase EpsE of Vibrio cholerae. *J. Mol. Biol.* (2003) doi:10.1016/j.jmb.2003.07.015.

49. Yeo, H. J., Savvides, S. N., Herr, A. B., Lanka, E. & Waksman, G. Crystal structure of the hexameric traffic ATPase of the *Helicobacter pylori* type IV secretion system. *Mol. Cell* (2000) doi:10.1016/S1097-2765(00)00142-8.

50. Jakovljevic, V., Leonardy, S., Hoppert, M. & Søgaard-Andersen, L. PilB and PilT are ATPases acting antagonistically in type IV pilus function in *Myxococcus xanthus*. *J. Bacteriol.* (2008) doi:10.1128/JB.01793-07.

51. Planet, P. J., Kachlany, S. C., DeSalle, R. & Figurski, D. H. Phylogeny of genes for secretion NTPases: Identification of the widespread tadA subfamily and development of a diagnostic key for gene classification. *Proc. Natl. Acad. Sci. U. S. A.* (2001) doi:10.1073/pnas.051436598.

52. Adams, D. W., Pereira, J. M., Stoudmann, C., Stutzmann, S. & Blokesch, M. The type IV pilus protein PilU functions as a PilT-dependent retraction ATPase. *PLoS Genet.* (2019) doi:10.1371/journal.pgen.1008393.

53. Whitchurch, C. B. & Mattick, J. S. Characterization of a gene, pilU, required for twitching motility but not phage sensitivity in *Pseudomonas aeruginosa*. *Mol. Microbiol.* (1994) doi:10.1111/j.1365-2958.1994.tb00499.x.

54. Park, H. S. M., Wolfgang, M. & Koomey, M. Modification of type IV pilus-associated epithelial cell adherence and multicellular behavior by the PilU protein of *Neisseria gonorrhoeae*. *Infect. Immun.* (2002) doi:10.1128/IAI.70.7.3891-3903.2002.

55. McCallum, M. *et al.* Multiple conformations facilitate PilT function in the type IV pilus. *Nat. Commun.* (2019) doi:10.1038/s41467-019-13070-z.

56. Chlebek, J. L. *et al.* PilT and PilU are homohexameric ATPases that coordinate to retract type IVa pili. *PLoS Genet.* (2019) doi:10.1371/journal.pgen.1008448.

57. Satyshur, K. A. *et al.* Crystal Structures of the Pilus Retraction Motor PilT Suggest Large Domain Movements and Subunit Cooperation Drive Motility. *Structure* (2007) doi:10.1016/j.str.2007.01.018.

58. Craig, L. *et al.* Type IV Pilus Structure by Cryo-Electron Microscopy and Crystallography: Implications for Pilus Assembly and Functions. *Mol. Cell* (2006) doi:10.1016/j.molcel.2006.07.004.

59. Nivaskumar, M. *et al.* Distinct docking and stabilization steps of the pseudopilus conformational transition path suggest rotational assembly of type IV pilus-like fibers. *Structure* (2014) doi:10.1016/j.str.2014.03.001.

60. Gold, V. & Kudryashev, M. Recent progress in structure and dynamics of dual-membrane-spanning bacterial nanomachines. *Current Opinion in Structural Biology* (2016) doi:10.1016/j.sbi.2016.03.001.

61. Lee, C. K. *et al.* Multigenerational memory and adaptive adhesion in early bacterial biofilm communities. *Proc. Natl. Acad. Sci. U. S. A.* (2018) doi:10.1073/pnas.1720071115.

62. Talà, L., Fineberg, A., Kukura, P. & Persat, A. *Pseudomonas aeruginosa* orchestrates twitching motility by sequential control of type IV pili movements. *Nature Microbiology* (2019) doi:10.1038/s41564-019-0378-9.

63. Chiang, P., Habash, M. & Burrows, L. L. Disparate subcellular localization patterns of *Pseudomonas aeruginosa* type IV pilus ATPases involved in twitching motility. *J. Bacteriol.* (2005) doi:10.1128/JB.187.3.829-839.2005.

64. L., C. J., Rémi, D., Lisa, C. & B., D. A. Motor-independent retraction of type IV pili is governed by an inherent property of the pilus filament. *Proc. Natl. Acad. Sci.* **118**, e2102780118 (2021).

65. Hoang, T. T., Karkhoff-Schweizer, R. R., Kutchma, A. J. & Schweizer, H. P. A broad-host-range F1p-FRT recombination system for site-specific excision of chromosomally-located DNA sequences: Application for isolation of unmarked *Pseudomonas aeruginosa* mutants. *Gene* (1998) doi:10.1016/S0378-1119(98)00130-9.

66. Herrero, M., V, de L. & Timmis, K. N. Transposon vectors containing non-antibiotic resistance selection markers for cloning and stable chromosomal insertion of foreign genes in gram-negative bacteria. *J. Bacteriol.* **172**, 6557–6567 (1990).

67. Hancock, R. E. & Carey, A. M. Outer membrane of *Pseudomonas aeruginosa*: heat-2-mercaptoethanol-modifiable proteins. *J. Bacteriol.* **140**, 902–910 (1979).

68. Jacobs, M. A. *et al.* Comprehensive transposon mutant library of *Pseudomonas aeruginosa*. *Proc. Natl. Acad. Sci. U. S. A.* (2003) doi:10.1073/pnas.2036282100.

69. Chiang, P. & Burrows, L. L. Biofilm formation by hyperpiliated mutants of Pseudomonas aeruginosa. *J. Bacteriol.* (2003) doi:10.1128/JB.185.7.2374-2378.2003.

70. Persat, A., Inclan, Y. F., Engel, J. N., Stone, H. A. & Gitai, Z. Type IV pili mechanochemically regulate virulence factors in *Pseudomonas aeruginosa*. *Proc. Natl. Acad. Sci. U. S. A.* **112**, 7563–7568 (2015).

71. Snyman, M., Huynh, T. V, Smith, M. T. & Xu, S. The genome-wide rate and spectrum of EMS-induced heritable mutations in the microcrustacean Daphnia: on the prospect of forward genetics. *Heredity (Edinb).* (2021) doi:10.1038/s41437-021-00478-x.

72. Andreoni, V., Bernasconi, S. & Bestetti, G. Biotransformation of ferulic acid and related compounds by mutant strains of *Pseudomonas fluorescens. Appl. Microbiol. Biotechnol.* **42**, 830–835 (1995).

73. Montie, T. C., Doyle-Huntzinger, D., Craven, R. C. & Holder, I. A. Loss of virulence associated with absence of flagellum in an isogenic mutant of *Pseudomonas aeruginosa* in the burned-mouse model. *Infect. Immun.* **38**, 1296–1298 (1982).

74. Govan, J. R. & Fyfe, J. A. Mucoid *Pseudomonas aeruginosa* and cystic fibrosis: resistance of the mucoid from to carbenicillin, flucloxacillin and tobramycin and the isolation of mucoid variants in vitro. *J. Antimicrob. Chemother.* **4**, 233–240 (1978).

75. Deatherage, D. E. & Barrick, J. E. Identification of mutations in laboratory-evolved microbes from next-generation sequencing data using breseq. *Methods Mol. Biol.* **1151**, 165–188 (2014).

76. Koo, J. *et al.* PilF is an outer membrane lipoprotein required for multimerization and localization of the *Pseudomonas aeruginosa* type IV pilus secretin. *J. Bacteriol.* (2008) doi:10.1128/JB.00996-08.

77. Asikyan, M. L., Kus, J. V & Burrows, L. L. Novel Proteins That Modulate Type IV Pilus Retraction Dynamics in *Pseudomonas aeruginosa*. *J. Bacteriol.* **190**, 7022–7034 (2008).

78. Kus, J. V, Tullis, E., Cvitkovitch, D. G. & Burrows, L. L. Significant differences in type IV pilin allele distribution among *Pseudomonas aeruginosa* isolates from cystic fibrosis (CF) versus non-CF patients. *Microbiology* **150**, 1315–1326 (2004).

79. Tammam, S. *et al.* PilMNOPQ from the *Pseudomonas aeruginosa* type IV pilus system form a transenvelope protein interaction network that interacts with PilA. *J. Bacteriol.* (2013) doi:10.1128/JB.00032-13.

80. Jones, C. J. & Wozniak, D. J. Congo Red Stain Identifies Matrix Overproduction and Is an Indirect Measurement for c-di-GMP in Many Species of Bacteria BT - c-di-GMP Signaling: Methods and Protocols. in (ed. Sauer, K.) 147–156 (Springer New York, 2017). doi:10.1007/978-1-4939-7240-1_12.

81. Pelham, R. J. & Wang, Y. Cell locomotion and focal adhesions are regulated by substrate flexibility. *Proc. Natl. Acad. Sci.* **94**, 13661–13665 (1997).

82. Sega, G. A. A review of the genetic effects of ethyl methanesulfonate. *Mutat. Res. Genet. Toxicol.* **134**, 113–142 (1984).

83. Kuchma, S. L. *et al.* Cyclic-di-GMP-mediated repression of swarming motility by *Pseudomonas aeruginosa*: the pilY1 gene and its impact on surface-associated behaviors. *J. Bacteriol.* **192**, 2950–2964 (2010).

84. S., W. S. *et al.* Force-Induced Changes of PilY1 Drive Surface Sensing by *Pseudomonas aeruginosa*. *MBio* **13**, e03754-21 (2022).

85. Nassif, X. *et al.* Roles of pilin and PilC in adhesion of *Neisseria meningitidis* to human epithelial and endothelial cells. *Proc. Natl. Acad. Sci. U. S. A.* **91**, 3769–3773 (1994).

86. Ma, C. *et al.* Bio-production of high-purity propionate by engineering l-threonine degradation pathway in *Pseudomonas putida*. *Appl. Microbiol. Biotechnol.* **104**, 5303–5313 (2020).

87. BURNS, G., BROWN, T., HATTER, K. & SOKATCH, J. R. Comparison of the amino

acid sequences of the transacylase components of branched chain oxoacid dehydrogenase of *Pseudomonas putida*, and the pyruvate and 2-oxoglutarate dehydrogenases of *Escherichia coli*. *Eur. J. Biochem.* **176**, 165–169 (1988).

88. Krueger, J. *et al.* Unravelling post-transcriptional PrmC-dependent regulatory mechanisms in *Pseudomonas aeruginosa*. *Environ. Microbiol.* **18**, 3583–3592 (2016).

89. Biais, N., Higashi, D., So, M. & Ladoux, B. Techniques to measure pilus retraction forces. *Methods Mol. Biol.* **799**, 197–216 (2012).

90. Kennouche, P. *et al.* Deep mutational scanning of the *Neisseria meningitidis* major pilin reveals the importance of pilus tip-mediated adhesion. *EMBO J.* **38**, e102145 (2019).

91. Ellison, C. K. *et al.* Retraction of DNA-bound type IV competence pili initiates DNA uptake during natural transformation in *Vibrio cholerae*. *Nat. Microbiol.* **3**, 773–780 (2018).

92. Floyd, K. A. *et al.* c-di-GMP modulates type IV MSHA pilus retraction and surface attachment in *Vibrio cholerae*. *Nat. Commun.* **11**, 1549 (2020).

93. Snyder, R. *et al.* Surface Sensing Stimulates Cellular Differentiation in *Caulobacter crescentus*. *Proc. Natl. Acad. Sci.* (2020) doi:10.1073/pnas.1920291117.

94. Ellison, C. K., Dalia, T. N., Dalia, A. B. & Brun, Y. V. Real-time microscopy and physical perturbation of bacterial pili using maleimide-conjugated molecules. *Nat. Protoc.* **14**, 1803–1819 (2019).

95. Ellison, C. K. *et al.* Obstruction of pilus retraction stimulates bacterial surface sensing. *Science (80-.).* (2017) doi:10.1126/science.aan5706.

96. Li, J., Egelman, E. H. & Craig, L. Structure of the *Vibrio cholerae* Type IVb Pilus and Stability Comparison with the *Neisseria gonorrhoeae* Type IVa Pilus. *J. Mol. Biol.* **418**, 47–64 (2012).

97. Ahmed, T., H., J. M., M., B. J. & J., B. T. Nanoscale Characterization and Determination of Adhesion Forces of *Pseudomonas aeruginosa* Pili by Using Atomic Force Microscopy. *J. Bacteriol.* **188**, 370–377 (2006).

CHAPTER 7. SUPPLEMENTARY DATA

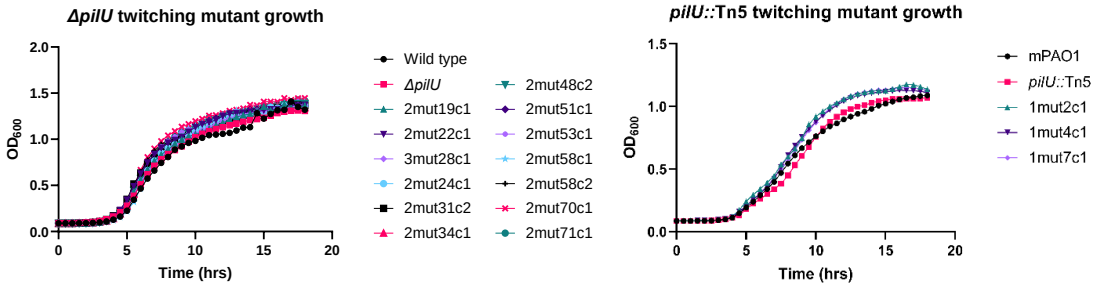

Supplementary Figure 1. Growth curves of gain-of-twitching mutants. There is no growth attenuation in the gain-of-twitching mutants. Subcultures were standardized to OD_{600} 0.1 and diluted to 1/1000. Cultures were incubated at 37°C for 18 h shaking at 200 rpm, and OD_{600} was measured every 30 min. N=6 technical replicates for *ΔpilU* mutants, N=16 technical replicates for *pilU::Tn5* mutants.

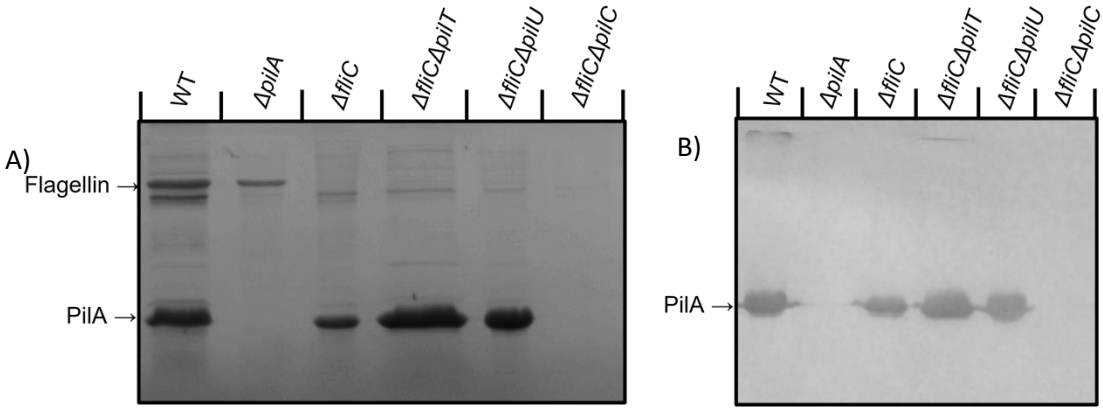

Supplementary Figure 2. SDS-PAGE and Western blot of PoMP strains. A) SDS-PAGE gel of surface shearing assay for PoMP strains. No Flagellin is visible on the gel but PilA is present for predicted piliated strains. B) Western blot for PilA from surface shearing assay of PoMP strains.

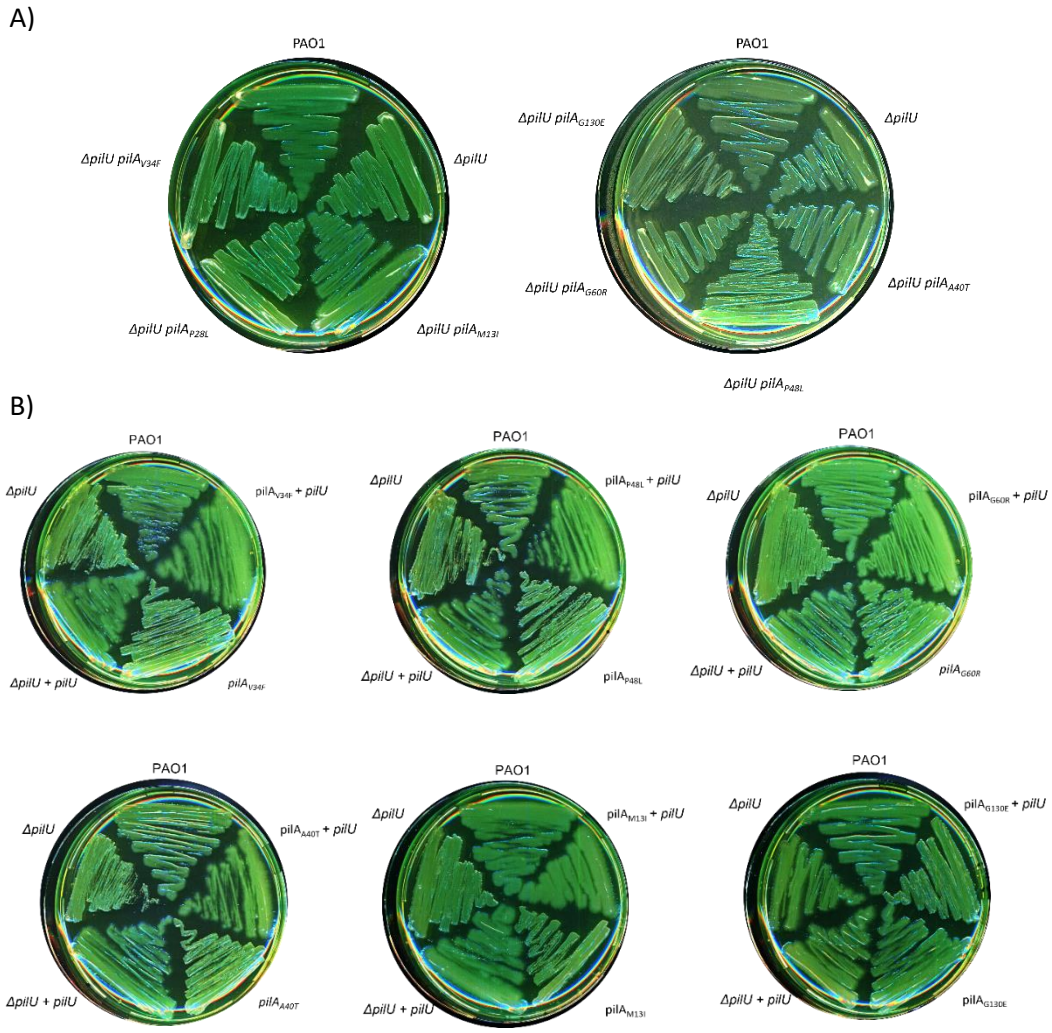

Supplementary Figure 3. Representative images of *P. aeruginosa ΔpilU pilA* point mutant colony morphology. A) Phenotypes of WT *P. aeruginosa* PAO1, *pilU*, and *pilU pilA* point mutant cultures. B) Phenotypes *pilU* and *pilU pilA* point mutant cultures complemented with *pilU* compared to WT *P. aeruginosa* PAO1 with an empty vector. Cells were streaked on LB agar and incubated at 37°C for 12 h prior to imaging with a flatbed scanner.